Optical phenomena in thin-film magnetic waveguides and their technical application

A. M. Prokhorov, G. A. Smolenskiĭ, and A. N. Ageev

Institute of General Physics of the Academy of Sciences of the USSR, Moscow;

A. F. Ioffe Institute of the Academy of Sciences of the USSR, Leningrad

Usp. Fiz. Nauk **143**, 33–72 (May 1984)

Research on waveguide magnetooptics is examined. A theory is presented of planar waveguides with dielectric permittivity and magnetic susceptibility taken into account. The properties of epitaxial films of ferrite garnets that determine their waveguide characteristics are discussed. Examples of functional elements of integrated optics that employ magnetic materials are given.

PACS numbers:

TABLE OF CONTENTS

INTRODUCTION

The problems involved in the widespread use of laser technology, both for practical purposes (communications, information processing, range-finding, etc.) and for physics research, have stimulated the development of a new field of technical physics—integrated optics.[1–4] Although its main problem has been to establish the principles for constructing planar integrated-optic circuits, the very phenomenon of waveguide propagation of light has proved useful both for studying fundamental problems of the interaction of light with matter and for studying the properties of surface layers and thin films, including those offering interest for a number of new fields of application. We note that when stress is placed on studying the physical phenomena in waveguides rather than on integration of optical elements into optical circuits, it is more expedient, following Ref. 4, to employ the term "waveguide" optics..

The propagation of light in the form of waveguide modes creates specific features and unique potentialities of the waveguide method, in particular for studying thin films.[5] We note also the features of waveguide optics such as the possibility of propagation of light in a film to distances far greater than its thickness, the obtaining of high densities of light energy, the discreteness of the attainable values of propagation constants, and the transverse energy distribution along the waveguide, etc. In addition to simultaneous highly accurate measurement of the thickness and refractive index of isotropic and homogeneous films, the method is employed for studying their inhomogeneities and also optical anisotropy and gyrotropy. The number of waveguide methods already developed up to now is large (see, e.g., Refs. 5–7). However, they are not yet employed widely enough.

This review is devoted to waveguide magnetooptics—a field of physical studies of waveguide structures containing magnetic materials that is a little more than ten years old. As the object of experimental study in this field, epitaxial films of ferrite garnets have been chosen. The technology of preparing them has developed in connection with potential applications in memory devices based on cylindrical magnetic domains and in UHF technology. They can find application also in integrated optics, apparently primarily as nonreciprocal elements of optical circuits such as isolators, circulators, etc. Although uncoupling elements can be designed also without using magnetic materials (see, e.g., Ref. 8), they will hardly be competitive with the magnetooptic elements. At present it is difficult to estimate the scales of employment, e.g., of nonreciprocal elements in future integrated-optic systems. The strong "noise" and oscillations of output power of a laser diode when coupled with a fibert[9] apparently show the need of using uncoupling elements, not only in fiber optics, but also in integrated optics. Such elements will be necessary first of all for hybrid and integrated-optic analog systems having small losses.

In addition to nonreciprocal elements, this review will briefly treat also other possible applications of magnetic materials in integrated optics.

Section 1 of this review will briefly treat the fundamental problems involved in the description of propagation of electromagnetic radiation in a magnetic material.

Section 2 will treat the phenomenon of waveguide propagation of light in magnetic films.

Section 3 is devoted to studying the properties of epitaxial films of garnets that govern their characteristics as waveguides.

In Sec. 4 we shall take up some concrete examples of employment of epitaxial films of ferrite garnets in integrated-optics elements.

 0038-5670/84/050339-24$01.80

1. MAXWELL'S EQUATIONS, MATERIAL RELATIONSHIPS, AND BOUNDARY CONDITIONS FOR MAGNETIC MEDIA AT OPTICAL FREQUENCIES

The propagation of electromagnetic waves in dielectric media is described by the averaged microscopic equations of Maxwell[10–17]:

$$\nabla\times\mathbf{E}=-\frac{1}{c}\frac{\partial\mathbf{B}}{\partial t},\quad \nabla\times\mathbf{B}=\frac{1}{c}\frac{\partial\mathbf{E}}{\partial t}+\frac{4\pi}{c}\mathbf{J},$$

$$\nabla\mathbf{B}=0,\quad \nabla\mathbf{E}=4\pi\rho. \tag{1}$$

Here **E** and **B** are the electric-field intensity and the magnetic induction of the electromagnetic wave, **J** and ρ are the current and the charge densities induced by the electromagnetic field, and c is the velocity of light in a vacuum.

Instead of the current densities and the charge, one often employs the two vectors $\vec{\mathscr{P}}$ and $\vec{\mathscr{M}}$.[10–12]

$$\mathbf{J}=\frac{\partial\vec{\mathscr{P}}}{\partial t}+c\nabla\times\vec{\mathscr{M}},\quad \rho=-\nabla\vec{\mathscr{P}}. \tag{2}$$

By using them, one can write Eq. (1) in the following form:

$$\nabla\times\mathbf{E}=-\frac{1}{c}\frac{\partial\mathbf{B}}{\partial t},\quad \nabla\times\mathbf{H}=\frac{1}{c}\frac{\partial\mathbf{D}}{\partial t},$$

$$\nabla\mathbf{B}=0,\quad \nabla\mathbf{D}=0. \tag{3}$$

Here the vectors **H** and **D** are defined by the relationships

$$\mathbf{H}=\mathbf{B}-4\pi\vec{\mathscr{M}}\quad\text{и}\quad \mathbf{D}=\mathbf{E}+4\pi\vec{\mathscr{P}}. \tag{4}$$

Although the vectors $\vec{\mathscr{P}}$ and $\vec{\mathscr{M}}$ unambiguously define the current and charge densities, as is evident from (2), they themselves are not defined unambiguously. The same is true of **H** and **D**. It will become clear below what the meaning of introducing these quantities is.

In order to make the system of equations (1) and (3) closed, one must relate the pairs of quantities **J** and ρ; $\vec{\mathscr{P}}$ and $\vec{\mathscr{M}}$, or **H** and **D** to the electric-field intensity and the magnetic induction, i.e., fix the material relationships. We shall study fields whose dependence on the coordinates and the time is defined by the function $\exp[i(\mathbf{k}\cdot\mathbf{r}-\omega t)]$. Within the framework of linear electrodynamics, the general material equations for a homogeneous, infinite medium can have the form[10]

$$\mathbf{D}=\hat{\varepsilon}(\omega,\mathbf{k})\mathbf{E},\quad \mathbf{B}=\hat{\mu}(\omega,\mathbf{k})\mathbf{H}. \tag{5}$$

Here $\hat{\varepsilon}$ and $\hat{\mu}$ are the effective dielectric-permittivity and magnetic-susceptibility tensors. The **D**(**B**) and **H**(**E**) relationships are contained implicitly in these material relationships.[16] As we have already noted above, the quantities **H** and **D**, and hence also $\hat{\varepsilon}$ and $\hat{\mu}$, are not defined unambiguously.[10] In each concrete case one can start with considerations of convenience of mathematical description and physical interpretation of the experimental results. One can always set $\mu_{ij}=\delta_{ij}$ (where δ_{ij} is the Kronecker symbol). Then the response of the medium to the action of the electromagnetic field will be described by the single effective tensor $\hat{\varepsilon}'(\omega,\mathbf{k})$. The dependence of this tensor on **k** is not necessarily associated with the spatial dispersion of $\hat{\varepsilon}(\omega,\mathbf{k})$ in (5), but may determine the local interaction of the medium with the magnetic component **B** or the magnetoelectric coupling.[16]

On the other hand, it is often recommended that one should avoid making such a separation[12,17] by employing a single effective dielectric permittivity tensor $\hat{\varepsilon}'(\omega,\mathbf{k})$, owing to the ambiguity of the separation of the current into two components. On the other hand, in certain cases it proves convenient to introduce the tensor $\hat{\mu}$ if this leads to retaining the boundary conditions in their usual form:

$$\begin{array}{ll}1)\ \mathbf{n}\times(\mathbf{E}_2-\mathbf{E}_1)=0, & 2)\ \mathbf{n}\times(\mathbf{H}_2-\mathbf{H}_1)=0,\\ 3)\ \mathbf{n}\cdot(\mathbf{B}_2-\mathbf{B}_1)=0, & 4)\ \mathbf{n}\cdot(\mathbf{D}_2-\mathbf{D}_1)=0.\end{array} \tag{6}$$

Here **n** is the unit vector normal to the phase boundary of the media 1 and 2. For example, these boundary conditions are kept to a sufficient degree of accuracy in the case of local coupling of $\vec{\mathbf{J}}$ with **E** and **B**,[13] or in the case of media having optical activity.[14] We shall restrict the treatment below to the former of these approximations. We shall write the material relationships in the following form:

$$4\pi\vec{\mathscr{P}}=(\hat{\varepsilon}(\omega)-1)\mathbf{E},\quad 4\pi\vec{\mathscr{M}}=(1-\mu^{-1}(\omega))\mathbf{B}. \tag{7}$$

We shall assume the interaction of the electromagnetic field with the medium to be local and neglect magnetoelectric coupling. The components of the tensors $\hat{\varepsilon}$ and $\hat{\mu}$ are determined respectively by the electric and magnetic dipole transitions. As is known,[15] even in this approximation the magnetic moment of the object is not determined by the vector $\vec{\mathscr{M}}$. The physical meaning of $\hat{\mu}(\omega)$ is ambiguous and can be elucidated only upon detailed study of the given material on the basis of microscopic models. As we have already noted above, rather than introducing the tensor $\hat{\mu}(\omega)$, one can employ the single tensor $\hat{\varepsilon}=(\omega,\mathbf{k})$. In the given approximation, the latter will contain terms quadratic in **k**.[16] Moreover, instead of the boundary conditions 2) and 4), we shall obtain the following from Eq. (6):

$$\begin{aligned}\mathbf{n}\times(\mathbf{H}_2'-\mathbf{H}_1')&=4\pi[\mathbf{n}\times(\vec{\mathscr{M}}_2-\vec{\mathscr{M}}_1)],\\ \mathbf{n}(\mathbf{D}_2'-\mathbf{D}_1')&=4\pi c[\mathbf{n}\cdot\nabla\times(\vec{\mathscr{M}}_2-\vec{\mathscr{M}}_1)].\end{aligned} \tag{8}$$

Here we have

$$\frac{\partial\mathbf{D}'}{\partial t}=\frac{\partial\mathbf{E}}{\partial t}+4\pi\frac{\partial\vec{\mathscr{P}}}{\partial t}+4\pi c\nabla\times\vec{\mathscr{M}},\quad \mathbf{H}'=\mathbf{B}.$$

Thus the tangential component of the vector **H**′ and the normal component of the vector **D**′ will not be continuous at the phase boundary of the media if $\vec{\mathscr{M}}\neq 0$.

The material presented above implies that the introduction of an effective dielectric permittivity tensor $\hat{\varepsilon}'(\omega)$ not dependent on **k** and the use of the ordinary boundary conditions, as is often done in waveguide magnetooptics, means that one neglects the interaction of the magnetic induction of the electromagnetic wave with the material. Apparently in the case of para- and ferromagnetics this is not always valid,[18] and taking it into account may lead to new effects in waveguide optics.[19] Of course, we should bear in mind the fact that effects involving the magnetic moment of molecules induced by the magnetic induction, the magnetoelectric coupling, and the spatial dispersion are small, and generally can be of the same order of magnitude. Therefore it is usually difficult to prove that a chosen interpretation of an experiment is the only one possible.[17] However, this does not mean

that it is impossible in principle to distinguish thse mechanisms in all cases.

We shall treat below the waveguide propagation of light, assuming $\hat{\varepsilon}$ and $\hat{\mu}$ to be independent of $\mathbf{k}$ [approximation (7)] and employing the boundary conditions (6).

Let us study the form of the tensor $\hat{\varepsilon}$ (analogous expressions hold for $\hat{\mu}$ in the general case) in a magnetically ordered dielectric. Without allowing for losses, the tensor $\hat{\varepsilon}$ is Hermitian, and it can be broken up into symmetric and antisymmetric parts:

$$\varepsilon_{ij} = \varepsilon_{ij}^{C} + i\varepsilon_{ij}^{A}. \tag{9}$$

Here the components ε_{ij}^{C} and ε_{ij}^{A} are real.

The symmetric part of the tensor can be written in matrix notation[20]:

$$\hat{\varepsilon}^{C} = \begin{bmatrix} \varepsilon_1 & \varepsilon_6 & \varepsilon_5 \\ \varepsilon_6 & \varepsilon_2 & \varepsilon_4 \\ \varepsilon_5 & \varepsilon_4 & \varepsilon_3 \end{bmatrix}. \tag{10}$$

The antisymmetric part can be written in terms of the components of the gyration pseudovector $\mathbf{a}$, the dual tensor $\hat{\varepsilon}^{A}$:

$$\hat{\varepsilon}^{A} = \begin{bmatrix} 0 & a_3 & -a_2 \\ -a_3 & 0 & a_1 \\ a_2 & -a_1 & 0 \end{bmatrix} \tag{11}$$

or by using the Levi-Civita pseudotensor $\delta_{ijk} = (i-j)(j-k)(k-i)/2$:

$$\varepsilon_{ij}^{A} = \delta_{ijk} a_k. \tag{12}$$

We shall use the symbol b_i for the components of the tensor $\hat{\mu}^{A}$.

In connection with the fact that epitaxial films usually exist in a stressed state owing to mismatch of the lattice parameters of the film and the substrate (see Sec. 3), we shall be interested in the tensor $\hat{\varepsilon}$ in the presence of deformation of the crystal.

Let us restrict the treatment to crystals of the cubic system, of class $m3m$ (O_h in Schoenflies notation), to which in particular the garnets belong. First let us take up the symmetric part of the tensor $\hat{\varepsilon}$. We can write the following expression for its components[21]:

$$\varepsilon_{ij}^{C} = \varepsilon_0 \delta_{ij} - \varepsilon_0^2 p_{ijkl} u_{kl} + g_{ijkl} M_k M_l + \ldots, \tag{13}$$

Here $\sqrt{\varepsilon_0} = n$ is the isotropic refractive index of the cubic crystal independent of magnetic ordering, and p_{ijkl}, u_{kl}, and g_{ijkl} are respectively the components of the photoelasticity and strain tensors and the magnetooptic tensor of second order in the magnetization, while the M_k are the components of the magnetization vector of the crystal.

The second term on the right-hand side of (13) describes the nonmagnetic birefringence involved, in the case of epitaxial films, with the mismatch of lattice parameters of the film and the substrate. The last term in (13) is of magnetic origin and describes effects involved with magnetostriction leading to macro- and microscopic lattice distortion[22] as well as the Voigt effect.[21] The effects involving macroscopic distortions are calculated by using the tensor $\hat{p}$ and the magnetostrictive constants. For garnets they prove to be two orders of magnitude smaller than the total contribution of the two other mechanisms.[23] Yet the separation of the contributions of the mechanisms involving microscopic distortions to the dielectric permittivity and responsible for the Voigt effect is as yet an unsolved problem.

As regards the antisymmetric part of the tensor $\hat{\varepsilon}$, it can be written in an approximation linear in the magnetization in the following form:

$$\varepsilon_{ij}^{A} = \delta_{ijk} f_{cr}^{\varepsilon} M_p. \tag{14}$$

Here the f_{cr}^{ε} are the components of the magnetooptic tensor of first order in the magnetization, which determine the Faraday effect.

Generally, formulas (14) and the magnetic part of (13) are valid for ferromagnets; in the case of ferrimagnets, to which the ferrite garnets belong, one must take the magnetic sublattices into account. The following expression gives the antisymmetric part of the tensor $\hat{\varepsilon}$ with transitions in the octahedral and tetrahedral sublattices taken into account:

$$\varepsilon_{ij}^{A} = \delta_{ijk} \left(f_{cr}^{a} M_p^{a} + f_{cr}^{di} M_p^{d}\right) + \ldots. \tag{15}$$

Here the superscripts a and d refer respectively to octahedral and tetrahedral ions.

Analogously one can write the contribution to the symmetric part of the dielectric-permittivity tensor:

$$\varepsilon_{ij}^{C} = g_{ijkl}^{a} M_k^{a} M_l^{a} + g_{ijkl}^{d} M_k^{d} M_l^{d} + \ldots. \tag{16}$$

One can find a more detailed discussion of the problems of magnetooptics in Refs. 24–26 and in the literature cited there.

In studying the waveguide propagation of light, we shall restrict the treatment to the case of transitions at one ion in one sublattice. That is, we shall use the expressions (13) and (14).

Let us study the form of the photoelasticity tensor $\hat{p}$ and of the magnetooptic tensors $\hat{g}$ and $\hat{f}$ for the case of crystals of the cubic system in class $m3m$. The cubic symmetry restricts the tensors $\hat{p}$ and $\hat{g}$ to three independent components.[20] We shall be interested in epitaxial films grown on substrates with planes parallel to {100}, {111}, and {110}, which we shall denote respectively as the cases 100, 111, and 110. We shall select the following systems of coordinates for these cases:

1) $x \parallel [100]$, $y \parallel [010]$, $z \parallel [001]$ for the case 100,
2) $x \parallel [111]$, $y \parallel [11\bar{2}]$, $z \parallel [\bar{1}10]$ for the case 111,
3) $x \parallel [1\bar{1}0]$, $y \parallel [110]$, $z \parallel [001]$ for the case 110. (17)

For the case 100, Eq. (13) has the following form (in matrix notation in expanded form):

$$\begin{bmatrix} \varepsilon_1 - \varepsilon_0 \\ \varepsilon_2 - \varepsilon_0 \\ \varepsilon_3 - \varepsilon_0 \\ \varepsilon_4 \\ \varepsilon_5 \\ \varepsilon_6 \end{bmatrix} = -\varepsilon_0^2 \begin{bmatrix} p_{11} & p_{12} & p_{12} & 0 & 0 & 0 \\ p_{12} & p_{11} & p_{12} & 0 & 0 & 0 \\ p_{12} & p_{12} & p_{11} & 0 & 0 & 0 \\ 0 & 0 & 0 & p_{44} & 0 & 0 \\ 0 & 0 & 0 & 0 & p_{44} & 0 \\ 0 & 0 & 0 & 0 & 0 & p_{44} \end{bmatrix} \begin{bmatrix} u_1 \\ u_2 \\ u_3 \\ u_4 \\ u_5 \\ u_6 \end{bmatrix} + \begin{bmatrix} g_{11} & g_{12} & g_{12} & 0 & 0 & 0 \\ g_{12} & g_{11} & g_{12} & 0 & 0 & 0 \\ g_{12} & g_{12} & g_{11} & 0 & 0 & 0 \\ 0 & 0 & 0 & g_{44} & 0 & 0 \\ 0 & 0 & 0 & 0 & g_{44} & 0 \\ 0 & 0 & 0 & 0 & 0 & g_{44} \end{bmatrix} \begin{bmatrix} \alpha_1^2 \\ \alpha_2^2 \\ \alpha_3^2 \\ 2\alpha_2\alpha_3 \\ 2\alpha_1\alpha_3 \\ 2\alpha_1\alpha_2 \end{bmatrix} M^2. \tag{18}$$

Here the α_i are the direction cosines of the magnetization.

By using the transformation matrices, one can easily go to the cases 111 and 110 upon employing the recommenda-

tions presented in Ref. 27. The components of the tensors $\hat{p}$ or $\hat{g}$ in the new coordinates will be expressed in terms of the components for the case 100:

$$p_{k'l'} = [Q_1^{k'}Q_1^{l'} + Q_2^{k'}Q_2^{l'} + Q_3^{k'}Q_3^{l'}]\, p_{11} + [Q_1^{k'}Q_2^{l'} + Q_2^{k'}Q_1^{l'} + Q_1^{k'}Q_3^{l'} + Q_3^{k'}Q_1^{l'} + Q_2^{k'}Q_3^{l'} + Q_3^{k'}Q_2^{l'}]\, p_{12} + [Q_4^{k'}Q_4^{l'} + Q_5^{k'}Q_5^{l'} + Q_6^{k'}Q_6^{l'}]\, p_{44}, \quad (19)$$

Here the Q_i^j are expressed in terms of the direction cosines of the new and old axes according to the table from Ref. 27 (p. 664).

As a result of using the transformation matrices, Eq. (19), and the table of coefficients Q_i^j from Ref. 27, one can derive the following for the case 111 (we shall write out only the photoelastic part):

$$\begin{bmatrix} \varepsilon_1-\varepsilon_0 \\ \varepsilon_2-\varepsilon_0 \\ \varepsilon_3-\varepsilon_0 \\ \varepsilon_4 \\ \varepsilon_5 \\ \varepsilon_6 \end{bmatrix} = -\varepsilon_0^2 \begin{bmatrix} p_{11}-2\Delta p/3 & p_{12}+\Delta p/3 & p_{12}+\Delta p/3 & 0 & 0 & 0 \\ p_{12}+\Delta p/3 & p_{11}-\Delta p/2 & p_{12}+\Delta p/6 & 0 & 0 & -\Delta p/3\sqrt{2} \\ p_{12}+\Delta p/3 & p_{12}+\Delta p/6 & p_{11}-\Delta p/3 & 0 & 0 & \Delta p/3\sqrt{2} \\ 0 & 0 & 0 & p_{44}+\Delta p/6 & \Delta p/3\sqrt{2} & 0 \\ 0 & 0 & 0 & \Delta p/3\sqrt{2} & p_{44}+\Delta p/3 & 0 \\ 0 & -\Delta p/3\sqrt{2} & \Delta p/3\sqrt{2} & 0 & 0 & p_{44}+\Delta p/3 \end{bmatrix} \begin{bmatrix} u_1 \\ u_2 \\ u_3 \\ u_4 \\ u_5 \\ u_6 \end{bmatrix}, \quad (20)$$

Here we have $\Delta p = p_{11} - p_{12} - 2p_{44}$. The magnetooptic part of the tensor ε^c has an analogous form. For the case 110 we have

$$\begin{bmatrix} \varepsilon_1-\varepsilon_0 \\ \varepsilon_2-\varepsilon_0 \\ \varepsilon_3-\varepsilon_0 \\ \varepsilon_4 \\ \varepsilon_5 \\ \varepsilon_6 \end{bmatrix} = -\varepsilon_0^2 \begin{bmatrix} p_{11}-\Delta p/3 & p_{12}+\Delta p/2 & p_{12} & 0 & 0 & 0 \\ p_{12}+\Delta p/2 & p_{11}-\Delta p/3 & p_{12} & 0 & 0 & 0 \\ p_{12} & p_{12} & p_{11} & 0 & 0 & 0 \\ 0 & 0 & 0 & p_{44} & 0 & 0 \\ 0 & 0 & 0 & 0 & p_{44} & 0 \\ 0 & 0 & 0 & 0 & 0 & p_{44}+\Delta p/2 \end{bmatrix} \begin{bmatrix} u_1 \\ u_2 \\ u_3 \\ u_4 \\ u_5 \\ u_6 \end{bmatrix}. \quad (21)$$

As the zero-order approximation, we shall employ the scalar quantity f instead of the gyrotropy tensor $\hat{f}$ by setting

$$\varepsilon_{ij}^A = f\,\delta_{ijk}M_k. \quad (22)$$

In closing this section, we shall give the solution of Maxwell's equation for an infinite, bigyrotropic (i.e., described by $\hat{\varepsilon}$ and $\hat{\mu}$) and anisotropic medium in the approximation (7). It can be represented in the form of the plane wave

$$\mathbf{A}(\mathbf{r}, t) = \mathbf{A}\exp[i(\mathbf{k}\cdot\mathbf{r} - \omega t)]. \quad (23)$$

Here $\mathbf{A}$ is taken to mean any of the fields, $\mathbf{E}$, $\mathbf{B}$, $\mathbf{D}$, or $\mathbf{H}$ that enter into (3) and (7). Upon solving the Maxwell's equations, one can obtain the following by selecting, as usual, $\mathbf{E}$ and $\mathbf{H}$ as the independent alternating fields:

$$\left[\begin{array}{ccc:ccc} \varepsilon_{22} & \gamma & -\beta & 0 & \varepsilon_{23} & \varepsilon_{21} \\ \gamma & \mu_{33} & \mu_{31} & \mu_{32} & 0 & 0 \\ -\beta & \mu_{13} & \mu_{11} & \mu_{12} & 0 & 0 \\ \hdashline 0 & \mu_{23} & \mu_{21} & \mu_{22} & -\gamma & \beta \\ \varepsilon_{32} & 0 & 0 & -\gamma & \varepsilon_{33} & \varepsilon_{31} \\ \varepsilon_{12} & 0 & 0 & \beta & \varepsilon_{13} & \varepsilon_{11} \end{array}\right] \left[\begin{array}{c} E_y \\ H_z \\ H_x \\ \hdashline H_y \\ E_z \\ E_x \end{array}\right] = 0. \quad (24)$$

Here we have $\beta = k_z/k_0$, $\gamma = k_x/k_0$, $k_0 = \omega/c = 2\pi/\lambda$, and λ is the wavelength of the light. In (24) the coordinate system is chosen such that the fields are homogeneous along the y axis, i.e., $k_y = 0$ in (23). The solutions of the system (24) are the eigenmodes of the bigyrotropic and anisotropic medium. Upon equating the determinant to zero, we obtain the equation[28]

$$\sum_{n=0}^{4} P_n(\beta)\,\gamma^n = 0. \quad (25)$$

This is of the fourth order in γ, and determines four plane waves (see Fig. 1) that can propagate in this system for a given value of β. We see from (24) that, when

$$\varepsilon_{12} = \varepsilon_{21} = \mu_{12} = \mu_{21} = \varepsilon_{23} = \varepsilon_{32} = \mu_{32} = \mu_{23} = 0 \quad (26)$$

the system breaks down into two independent systems that correspond to the linearly polarized TE ($E_yH_zH_x$) and TM ($H_yE_zE_x$) waves. The $P_n(\beta)$ in (25) are polynomials in β from the fourth to the zero order.[28]

2. PROPAGATION OF LIGHT IN PLANAR MAGNETOOPTIC ANISOTROPIC WAVEGUIDES

The optical phenomena that occur in the propagation of light in a waveguide in which at least one of the media (the substrate, the film, or the top layer) is magnetooptic have generally been treated in terms of the effective dielectric-permittivity tensor with the usual boundary conditions (6). On the basis of the material presented in Sec. 1, evidently the results of these studies are valid whenever magnetic polarization arising from the magnetic induction is absent. Another approach has been developed in Refs. 19, 28–30. In Ref. 29, the tensor $\hat{\varepsilon}$ was replaced with a scalar, while the

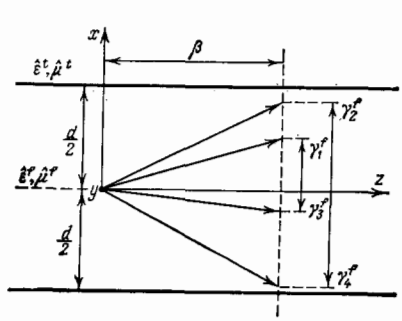

FIG. 1. Three-layer waveguide structure with the lower layer having $\hat{\varepsilon}^s\hat{\mu}^s$.

magnetooptic effects were taken into account by using a magnetic-susceptibility tensor with diagonal terms equal to unity. This method of description was justified by the contradictions that the authors faced when using the effective dielectric-permittivity tensor to describe the conversions among the asynchronous modes with the aid of diffraction grating. Without justification they stated that the contradictions involve the fact that the effective dielectric-permittivity tensor does not describe the magnetic effects. The arguments presented in Sec. 1 imply that the effective dielectric-permittivity tensor does not describe the magnetic effects associated with $\hat{\mu}$ if one uses the ordinary boundary conditions instead of (8).

In Refs. 19, 28, and 30 the waveguide propagation of light was discussed on the basis of the dipole-transition approximation of (7) (see Sec. 1). That is, both the permittivity and the susceptibility tensors were taken into account without allowing for the effects of spatial dispersion and magnetoelectric coupling. In the treatment below of propagation of radiation in gyrotropic and anisotropic waveguides, we shall also use this approximation with the boundary conditions (6).

The analysis of the phenomena in such waveguides can be based on several approximate methods. Some of them use the geometric-optics approximation without[31a] or with[31b] the Goos-Haenchen effect being taken into account, while others have treated the normal[32] or coupled[33–35] modes. Exact solutions can also exist,[28,36–39] which in complex cases (when the condition (26) does not hold) require using a computer.

Let us study an inhomogeneous, layered medium (Fig. 1). It is homogeneous in the y and z directions, while jumps exist in the x direction in the values of the components of the tensors $\hat{\varepsilon}$ and $\hat{\mu}$ at the phase boundaries $x = \pm d/2$. It is assumed that all three media (the top layer t, the film f, and the substrate s) are absolutely transparent ($\hat{\varepsilon}$ and $\hat{\mu}$ are Hermitian) and the thickness of the film is of the order of the wavelength of the light ($d \sim \lambda$). We shall be interested in the guided modes in such a structure, i.e., the light propagating in the film and near it. In order to satisfy the boundary conditions, the radiation must have the same value of β from (24). Hence the film will contain a combination of four waves (in the general case with differing values of γ), and only two waves in the substrate and two in the top layer.

Upon using (24) and the boundary conditions (6) for the y and z components of the **E** and **H** fields for the two phase boundaries, we can derive the following system of equations for determining the fields:

$$\begin{bmatrix} \lambda_1 & \lambda_2 & \lambda_3 & \lambda_4 & 0 & 0 & 1 & 1 \\ \lambda_1 e^f_{1z} & \lambda_2 e^f_{2z} & \lambda_3 e^f_{3z} & \lambda_4 e^f_{4z} & 0 & 0 & e^t_{1z} & e^t_{2z} \\ \lambda_1 h^f_{1z} & \lambda_2 h^f_{2z} & \lambda_3 h^f_{3z} & \lambda_4 h^f_{4z} & 0 & 0 & h^t_{1z} & h^t_{2z} \\ \lambda_1 h^f_{1y} & \lambda_2 h^f_{2y} & \lambda_3 h^f_{3y} & \lambda_4 h^f_{4y} & 0 & 0 & h^t_{1y} & h^t_{2y} \\ 1 & 1 & 1 & 1 & 1 & 1 & 0 & 0 \\ e^f_{1z} & e^f_{2z} & e^f_{3z} & e^f_{4z} & e^s_{1z} & e^s_{2z} & 0 & 0 \\ h^f_{1z} & h^f_{2z} & h^f_{3z} & h^f_{4z} & h^s_{1z} & h^s_{2z} & 0 & 0 \\ h^f_{1y} & h^f_{2y} & h^f_{3y} & h^f_{4y} & h^s_{1y} & h^s_{2y} & 0 & 0 \end{bmatrix} \begin{bmatrix} E^f_{y1}\sqrt{\lambda_1} \\ E^f_{y2}\sqrt{\lambda_2} \\ E^f_{y3}\sqrt{\lambda_3} \\ E^f_{y4}\sqrt{\lambda_4} \\ E^s_{y1}\lambda^s_1 \\ E^s_{y2}\lambda^s_2 \\ E^t_{y1}\lambda^t_1 \\ E^t_{y2}\lambda^t_2 \end{bmatrix} = 0. \tag{27}$$

Here we have $\lambda_n = \exp(-i\gamma^f_n d)$, $\lambda^s_n = \exp(i\gamma^s_n d/2)$, and $\lambda^t_n = \exp(i\gamma^t_n d/2)$, while the coefficients e and h are determined by the components of $\hat{\varepsilon}$ and $\hat{\mu}$ and depend on β.

The values of β_m (where m is the order of the mode) that make the determinant of the system (27) vanish determine the propagation constants of the guided modes. When (26) is satisfied, the modes can be linearly polarized (TE or TM). Otherwise the modes can be elliptically polarized (in particular, circularly polarized). Each such hybrid mode will be a linear combination of four solutions of the system (24) that differ in the general case in magnitude and direction of the waveguide eigenvectors (see Fig. 1). General restrictions have been obtained[40] (vanishing of certain components of $\hat{\varepsilon}$ and $\hat{\mu}$) that the authors deemed necessary to make possible propagation of radiation in a gyroanisotropic waveguide. False assumptions were made here that propagation requires fulfillment of the following equalities: $|\gamma^f_1| = |\gamma^f_3|$, and $|\gamma^f_2| = |\gamma^f_4|$. In fact there is no need of them. The vanishing of the determinant of the system (27) imposes no general restrictions on the form of the permittivity and susceptibility tensors.

At the same time, there are certain relationships between the components of the permittivity and susceptibility tensors in the film, on the one hand, and in the substrate and top layer, on the other, that are necessary for propagation of light in the waveguide. In lossless media one can treat a wave as being guided under the condition that the component of the time-averaged Poynting vector normal to the phase boundary vanishes and the fields vanish with increasing distance from the film. The Poynting vector in the approximation (7) is represented by the expression[41]

$$\mathbf{S} = \frac{c}{4\pi}[\mathbf{E} \times \mathbf{H}]. \tag{28}$$

The condition $\mathbf{s} \times \mathbf{x}_0 = 0$, where $\mathbf{x}_0$ is a unit vector along the x axis (Fig. 1), implies that the propagation constant ($k_0\beta_m$) or the effective refractive index of the mode (β_m) must be real. The condition at infinity require that $\operatorname{Im}\gamma^s_{1,2} > 0$ and $\operatorname{Im}\gamma^t_{1,2} < 0$, which imposes restrictions on the minimal possible values of β_m. All these conditions govern the waveguide propagation of light.[36]

For a completely isotropic waveguide structure, the condition for propagation is reduced to the requirement that

$$n^s \text{ and } n^t < \beta_m < n^f. \tag{29}$$

Whenever at least one of the media of the waveguide is anisotropic, the condition for propagation becomes more complex and becomes multivariant. Let us study the important case in which all three media amount to a biaxial crystal (we assume that $\mu_{ij} = \delta_{ij}$) whose principal dielectric axes coincide with the coordinate axes in Fig. 1. Then the symmetric part of the dielectric-permittivity tensor $\hat{\varepsilon}^c$ will be diagonal in these axes with $\varepsilon_1 \neq \varepsilon_2 \neq \varepsilon_3$. In this case Eq. (25) breaks down into two equations:

$$\begin{aligned} \gamma^2 &= \varepsilon_2 - \beta^2 && \text{for TE-polarization,} \\ \gamma^2 &= \varepsilon_3(\varepsilon_1 - \beta^2)/\varepsilon_1 && \text{for TM-polarization.} \end{aligned} \tag{30}$$

We can easily derive from this a condition for waveguide propagation having the form

$$\begin{aligned}&\sqrt{\varepsilon_2^s} \text{ and } \sqrt{\varepsilon_2^t} < \beta_m < \sqrt{\varepsilon_2^f} \quad \text{for TE-modes,}\\ &\sqrt{\varepsilon_1^s} \text{ and } \sqrt{\varepsilon_1^t} < \beta_m < \sqrt{\varepsilon_1^f} \quad \text{for TM-modes.}\end{aligned} \tag{31}$$

One can draw from these conditions the conclusion, important from a practical standpoint, that one can build a waveguide in which only waves of a single polarization can propagate. This is a so-called waveguide of the "semileaky" type.[42-44] The name involves the fact, that when a TE⇄TM mode conversion exists, the wave propagating in it (say TE) will "leak out" of the waveguide as it is converted into the TM mode, while it will propagate in it if not converted. Such a waveguide requires fulfillment of the condition

$$\varepsilon_1^f < \varepsilon_1^s \text{ and } \varepsilon_1^t, \text{ but } \varepsilon_2^f > \varepsilon_2^s \text{ and } \varepsilon_2^t$$

or

$$\varepsilon_2^f < \varepsilon_2^s \text{ and } \varepsilon_2^t, \text{ but } \varepsilon_1^f > \varepsilon_1^s \text{ and } \varepsilon_1^t. \tag{32}$$

In the former case the TE-mode is a guided mode while the TM mode is "leaky", and vice versa in the latter case. Thus the former structure can be used to design TE isolators, and the latter for TM isolators.

Now let us proceed to study other important properties of gyroanisotropic waveguides, namely the possibility of obtaining phase synchronization of modes in anisotropic structures and nonreciprocal propagation of radiation in the presence of gyrotropy.

As we have already pointed out above, in addition to the exact solutions of the problem of waveguide propagation of light, e.g., based on solving the system (27), there are approximate methods that employ the smallness of the nondiagonal terms of the permittivity and susceptibility tensors. Let us use one of these methods, namely the method of coupled modes,[33-35] with which we shall obtain analytic expressions useful for understanding the phenomena in magnetooptic anisotropic waveguides. In the zero-order approximation, it is useful to set

$$\varepsilon_{ij}(x) = \begin{cases} \varepsilon_0(x) & \text{when } i=j,\\ 0 & i \neq j,\end{cases}$$

$$\mu_{ij}(x) = \begin{cases} 1 & i=j,\\ 0 & i \neq j.\end{cases} \tag{33}$$

The solution of the waveguide problem in this approximation is well known (see, e.g., Ref. 29). The eigensolutions are the linearly polarized TE and TM modes. Figure 2 shows the calculated $\beta(d)$ relationship for the typical values of the refractive indices of the ferrite garnet film ($n^f = 2.220$), for the gadolinium gallium garnet substrate ($n^s = 1.945$), and wavelength $\lambda = 1.15\,\mu$m. We see from the graph that the values of β for the TE and TM modes of the same order (for the same m) for a given thickness are not equal to one another, but asymptotically approach one another with increasing film thickness. At thicknesses less than $\sim 0.2\,\mu$m, as we see, propagation of light in such a system is impossible. This arises from the asymmetry of the waveguide ($n^s \neq n^t$); fulfillment of the differing boundary conditions at the two boundaries requires too sharp a variation in the field inside the film. If one uses films thinner than $0.2\,\mu$m, then one must use a top layer having a refractive index close to that of the substrate.

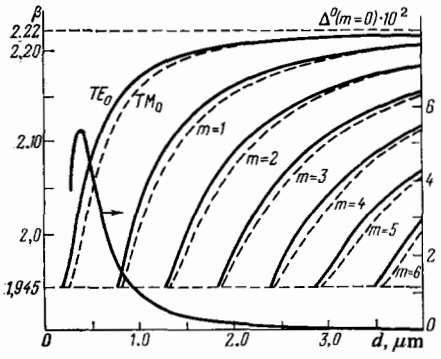

FIG. 2. Dependence of the effective refractive indices of the modes in an isotropic waveguide structure on the film thickness. Calculation with the parameters: $n^f = 2.22$, $n^s = 1.945$, $n^t = 1$, $\lambda = 1.15\,\mu$m.

In practice the situation often happens that one can restrict the treatment to only two modes with sufficiently close values of the propagation constants $k_0\beta_m$ without taking into account the existence of other modes, even if in principle they can propagate in the given waveguide. We shall restrict the treatment below to the two-mode approximation.

Let us assume that the two modes being studied in the zero-order approximation are modes of differing polarization, but of the same order (the most probable case in practice). Then we can write the following expression for the y component of the field in the TE mode:

$$E_y^0(x, z, t) = \frac{1}{2}\mathscr{E}(x)\exp[i(\beta_e^0 z - \omega t)] + \text{c.c.} \tag{34a}$$

and in the TM mode:

$$H_y^0(x, z, t) = \frac{1}{2}\mathscr{H}(x)\exp[i(\beta_h^0 z - \omega t)] + \text{c.c.} \tag{34b}$$

Here c. c. denotes the complex conjugate of the first term on the right-hand side, while the β_i^0 are the values of the effective refractive indices of the modes in the structure having the parameters of (33). The distances here are measured in units of $\lambda = \lambda/2\pi$. The difference (mismatch)

$$\Delta^0 = \beta_e^0 - \beta_h^0 \tag{35}$$

is always positive for TE_m and TM_m modes of the same order. Figure 2 shows the $\Delta^0(d)$ relationship for the zero-order modes.

Let us study the effect of a perturbation (anisotropy and gyrotropy) on the characteristics of the light in the waveguide. The appearance of nonzero values of the quantities $\varepsilon_{ii} - \varepsilon_0$, ε_{13}, ε_{31}, μ_{13}, and μ_{31} alters the propagation constants of the TE and TM modes by the amounts $k_0\delta_e$ and $k_0\delta_h$, respectively[19,30]:

$$\begin{aligned}\delta_e^{\pm} &= \langle(\varepsilon_2 - \varepsilon_0)\mathscr{E}^2\rangle \mp 2\beta_e^0\left\langle b_2\mathscr{E}\frac{d\mathscr{E}}{dx}\right\rangle,\\ \delta_h^{\pm} &= (\beta_h^0)^2\left\langle\frac{\varepsilon_1-\varepsilon_0}{\varepsilon_0^2}\mathscr{H}^2\right\rangle + \left\langle\frac{\varepsilon_3-\varepsilon_0}{\varepsilon_0^2}\left(\frac{d\mathscr{H}}{dx}\right)^2\right\rangle\\ &\quad \mp 2\beta_h^0\left\langle\frac{a_2}{\varepsilon_0^2}\mathscr{H}\frac{d\mathscr{H}}{dx}\right\rangle.\end{aligned} \tag{36}$$

Here we have adopted the notation

$$\langle A\rangle = \int_{-\infty}^{\infty} A(x)\,dx,$$

and have used the normalization conditions $2\beta_h^0\langle\varepsilon_0^{-1}\mathscr{H}^2\rangle = 2\beta_e^0\langle\mathscr{E}^2\rangle = 1$ and assumed $\mu_{ii} = 1$. The upper

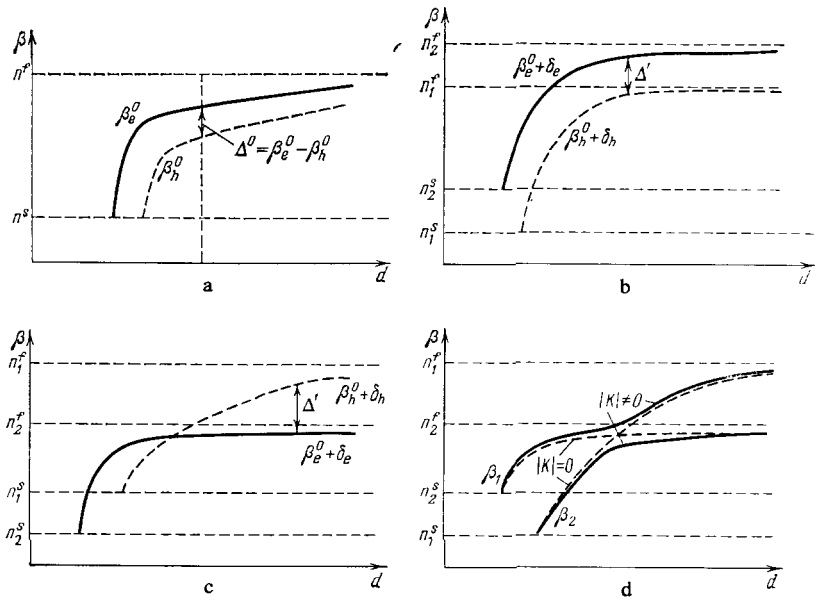

FIG. 3. Mode spectra for the following structures: a) isotropic; b) film and substrate are negative uniaxial crystals; c) film and substrate are positive crystals; d) transition from linearly polarized to hybrid modes.

and lower signs in (36) pertain to the two opposite directions of propagation of light.

Just as in the isotropic case, the modes remain linearly polarized, and there is no conversion among them. The mismatch now will be determined by the quantity

$$\Delta' = \Delta^0 + \delta_e - \delta_h. \tag{37}$$

Figure 3 shows the possible variations in the spectrum of the modes.[45] To obtain phase synchronization ($\Delta' = 0$), we must have $\delta_h > \delta_e$; upon taking into account the fact that the corrections δ are mainly governed by the first terms on the right-hand side of (36), we obtain the following condition for synchronization of modes:

$$(\beta_h^0)^2 \left\langle \frac{\varepsilon_1 - \varepsilon_0}{\varepsilon_0^2} \mathcal{H}^2 \right\rangle - \langle (\varepsilon_2 - \varepsilon_0)\, \mathcal{E}^2 \rangle = \Delta^0. \tag{38}$$

As we see from Fig. 3, anisotropy in the substrate or the top layer has a greater effect on the modes near the cutoff, but the anisotropy of the film does so far from cutoff.

We see from (36) that the shift in the TE mode depends linearly on the component b_2 of the tensor $\hat{\mu}$, while the shift in the TM mode depends on the component a_2 of the tensor $\hat{\varepsilon}$. In principle this makes it possible to measure the value of the gyration vectors of the tensors $\hat{\varepsilon}$ and $\hat{\mu}$ separately from the shifts in the corresponding modes upon remagnetizing the film along the y axis.[19] Figure 4 shows the dependence of the integrals governing these shifts on the thickness of the film.

Finally, if we take into account the nondiagonal terms of the tensors $\hat{\varepsilon}$ and $\hat{\mu}$ that enter into (26), we find, in contrast to the foregoing, that it becomes possible to convert one mode into the other as they propagate. This means that the linearly polarized modes are no longer eigenmodes of such a waveguide. The latter prove to be hybrid modes, having elliptical polarization in the general case. If we conduct the treatment in terms of coupled modes, then their spectrum remains the same as without taking into account the tensors that govern the conversion, but their amplitude varies as they propagate. Instead of (34), the y components of the fields will be

$$E_y(x, z, t) = \frac{1}{2} e(z)\, E_y^0(x, z, t) + \text{c.c.},$$
$$H_y(x, z, t) = \frac{1}{2} h(z)\, H_y^0(x, z, t) + \text{c.c.} \tag{39}$$

Here the slowly varying amplitudes e and h are determined by the coupled-mode equation[34]:

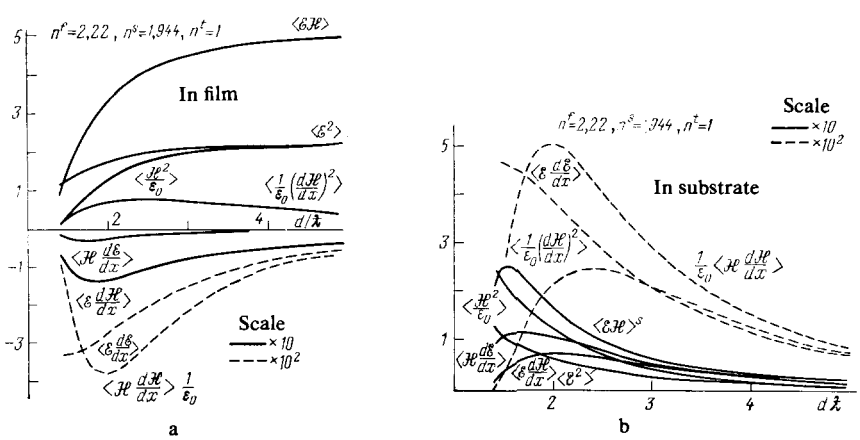

FIG. 4. Dependence of the overlap integrals on the reduced thickness d/λ. a) In the film; b) in the substrate. Parameters: $n^f = 2.22$, $n^s = 1.944$.

$$\frac{de'}{dz} = kh'e^{-i\Delta' z}, \quad \frac{dh'}{dx} = -k^* e' e^{i\Delta' z}, \tag{40}$$

where we have

$$e' = e(z)\, e^{-i\delta_e z} \quad \text{и} \quad h' = h(z)\, e^{-i\delta_h z}.$$

The conversion coefficient of the coupled modes (ratio of the square of the amplitude of the converted mode to the sum of squares of the amplitudes for both modes) is given by the expression

$$R(z) = \frac{|k|^2}{\nu^2} \sin^2 \nu z, \tag{41}$$

where we have

$$\nu = \sqrt{|k|^2 + (\Delta'/2)^2}.$$

The coupling coefficient k is determined by the expression

$$k = -\left\langle \frac{\varepsilon_{23}}{\varepsilon_0} \mathscr{E} \frac{d\mathscr{H}}{dx} \right\rangle - \left\langle \mu_{32} \mathscr{H} \frac{d\mathscr{E}}{dx} \right\rangle - i\beta_e^0 \langle \mu_{42} \mathscr{H} \mathscr{E} \rangle + i\beta_h^0 \left\langle \frac{\varepsilon_{21}}{\varepsilon_0} \mathscr{E} \mathscr{H} \right\rangle. \tag{42}$$

As we see from (41), the maximum conversion ($R = 1$) can occur only when $\Delta' \ll |k|$. It will occur at the distance (in real length units)

$$l = \frac{\lambda}{4|k|}. \tag{43}$$

If we treat the phenomenon in terms of hybrid modes with amplitudes invariant in the process of propagation, then they will have the following effective refractive indices[34]:

$$\beta_{\text{hybrid}}^{\pm} = \bar{\beta} \pm \nu, \tag{44}$$

Here we have $\bar{\beta} = (1/2)(\beta_e^0 + \delta_e + \beta_h^0 + \delta_h)$.

As we see from (44) (see Fig. 3), the curves of the refractive indices of the hybrid modes do not intersect, but approach at points of phase synchronization ($\Delta' = 0$).

As Eqs. (36) and (40) imply, the components of the tensors $\hat{\varepsilon}$ and $\hat{\mu}$ arising from optical anisotropy $\varepsilon_4, \mu_4, \varepsilon_6$, and μ_6, and also those arising from gyrotropy a_1, b_1, a_3, and b_3, govern the coupling coefficient, while the diagonal components of $\hat{\varepsilon}$ and a_2 and b_2, which arise from gyrotropy, govern the shift in the modes.

The possibility of obtaining nonreciprocal mode conversion is of especial importance for practical application (see Sec. 4) of waveguides containing magnetic media. One should try to have the conversion coefficient equal to zero ($R^+ = 0$) in propagation of light in one direction (say forward), and unity ($R^- = 1$) in the backward direction. The nonreciprocity of the conversion coefficient R can be associated with nonreciprocity of either the coupling coefficient k of (42) or of the mismatch Δ' of (37). We see from (41) that nonreciprocity in them will lead to nonreciprocity of the conversion coefficient. Let us study in turn the possible reasons for nonreciprocity of the coupling coefficient and the mismatch.

We can show from Maxwell's equation that the solution for a mode propagating, say, in the backward direction can be obtained by the operation of time reversal ($t \to -t$). As we know, this is equivalent to reversal of the magnetization ($\mathbf{M} \to -\mathbf{M}$). Usually it is more convenient, both in the theoretical and the experimental study of nonreciprocity to employ reversal of magnetization, rather than of direction of propagation. We can show from (42) that

$$\begin{aligned} \operatorname{Re} k^{\pm} &= -\left\langle \frac{\varepsilon_4}{\varepsilon_0} \mathscr{E} \frac{d\mathscr{H}}{dx} \right\rangle - \left\langle \mu_4 \mathscr{H} \frac{d\mathscr{E}}{dx} \right\rangle \mp \left\langle \left(\beta_h^0 \frac{a_3}{\varepsilon_0} + \beta_e^0 b_3 \right) \mathscr{E} \mathscr{H} \right\rangle, \\ \operatorname{Im} k^{\pm} &= \left\langle \left(\beta_h^0 \frac{\varepsilon_6}{\varepsilon_0} + \beta_e^0 \mu_6 \right) \mathscr{E} \mathscr{H} \right\rangle \pm \left\langle \frac{a_1}{\varepsilon_0} \mathscr{E} \frac{d\mathscr{H}}{dx} \right\rangle \mp \left\langle b_1 \mathscr{H} \frac{d\mathscr{E}}{dx} \right\rangle. \end{aligned} \tag{45}$$

Hence we see that nonreciprocity of the modulus of the coupling coefficient requires a combination of optical anisotropy, as determined by the symmetric part of the tensors $\hat{\varepsilon}$ and $\hat{\mu}$, and gyrotropy, which is described by the antisymmetric part of these tensors. In order to obtain the minimal coupling coefficient in propagation in the forward direction, the sign-variant and the constant terms in (45) must mutually compensate. Moreover, these terms separately must have as large values as possible in order to obtain the maximum possible value of $|k^-|$. Here we must not forget that Δ' should be minimal.

Figure 4 shows the dependence of the integrals entering into (45) on the thickness of the film. While the integrals $\langle \mathscr{E} \mathscr{H} \rangle$ increase monotonicaly upon going away from the cutoff of the modes, the integrals containing derivatives are substantial near the cutoff. Unfortunately the magnitude of Δ^0 near the cutoff is so large (see Fig. 2) that it cannot be compensated, neither by photoelasticity, nor *a fortiori* by the magnetooptics of the ferrite film (see Sec. 3). One can find an escape from this situation by using periodic structures (see below), strongly anisotropic top layers, or by going over to two-layer films. We shall return to this problem below.

Now let us turn to another possibility of obtaining nonreciprocal conversion, namely by nonreciprocal phase mismatch of the coupled modes as determined by the expressions (36). As we have already noted above, the mismatch depends linearly on the components of the gyration vectors when the latter are oriented along the y axis, i.e., perpendicular to the direction of propagation in the plane of the film (equatorial geometry). This problem has been treated theoretically in Refs. 28, 38, and 46 for the case of zero-order modes. Figure 5 shows the calculated dependence of the dis-

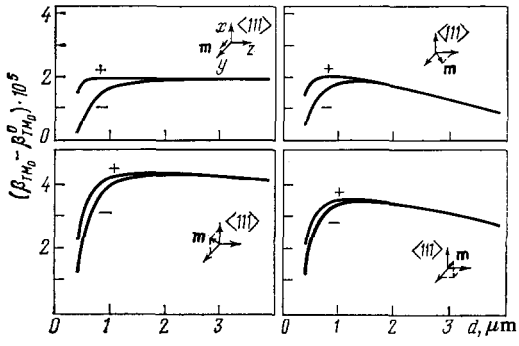

FIG. 5. Dependence of the displacement of the TM mode to the film thickness for the forward and backward waves.[28] Parameters: $n^f = 2.14$, $n^s = 1.94$, $n^t = 1$, $2g_{44}M^2 = 2.3 \cdot 10^{-4}$, $\Delta g M^2 = -0.4 \cdot 10^{-4}$, $g_{12}M^2 = 10^{-4}$.

placement of the modes for opposite directions of propagation of light. We see from the graphs that the effect is substantial only near the cutoff of the modes when the magnitudes of the integrals $\langle \mathscr{E} d\mathscr{E}/dx \rangle$ or $\langle \mathscr{H} d\mathscr{H}/dx \rangle$ become appreciable (see Fig. 4). Thus, in the case of nonreciprocal mismatch, just as when one employs nonreciprocity of the coupling coefficient, difficulties arise owing to the large magnitude of the detuning Δ^0 near the cutoff of the modes. This problem can be solved by using periodic structures or two-layer films.

In order to proceed to treat concrete waveguide structures, we must derive expressions for the components of the tensors $\hat{\varepsilon}$ and $\hat{\mu}$ in explicit form. We shall first take up the anisotropy due to photoelasticity. From the macroscopic standpoint, the deformation in the film resembles the deformation of a plate upon thermal expansion (or contraction) when one of its side faces is immobilized. As has been shown,[47] the stresses in such a plate are homogeneous stretching (or compressive) stresses lying in the plane of the plate, apart from its edges, where other stresses arise: inhomogeneous shear stresses and stresses perpendicular to the phase boundary. The latter disappear upon going several plate thicknesses away from the edges. Study of epitaxial films has shown that the strain in them can be considered elastic (see Sec. 3).

Upon neglecting edge effects, we can assume $u_4 = u_5 = u_6 = 0$. We shall assume (see Sec. 3) that the deformation in the film along the y and z axes is the same:

$$u_2 = u_3 \equiv u_{\parallel}. \tag{46}$$

We obtain from the vanishing of the stresses perpendicular to the film the following expression for the coupling of the strain $u_1 \equiv u_\perp$ with the strain in the plane of the film:

$$u_\perp = -hu_{\parallel}. \tag{47}$$

For the three cases of orientation of the crystallographic axes, we have the following expressions for the parameter h:

$$\text{a) } h_{100} = \frac{2c_{12}}{c_{11}}, \quad \text{b) } h_{111} = 2\frac{3c_{12}+\Delta c}{3c_{11}-2\Delta c}, \quad \text{c) } h_{110} = \frac{4c_{12}+\Delta c}{2c_{11}-\Delta c}. \tag{48}$$

Here we have $\Delta c = c_{11} - c_{12} - 2c_{44}$, and the c_{ij} are the components of the fourth-order stiffness-constant tensor (in matrix notation) that relates the stresses to the strain:

$$\sigma_i = c_{ij}u_j. \tag{49}$$

Here and below, we shall assume tensile strain and stresses to be positive, as is assumed in the theory of elasticity and is currently recommended also for the theory of photoelasticity. Previously the latter theory had usually adopted compressive stresses as being positive. In this case we should put a minus sign before the coefficients c_{ij} in (49).

Upon employing (18), (20), (21), and (47), we obtain the following expression for $\hat{\varepsilon}^C$ arising from photoelasticity:

$$\begin{bmatrix} \varepsilon_1-\varepsilon_0 \\ \varepsilon_2-\varepsilon_0 \\ \varepsilon_3-\varepsilon_0 \\ \varepsilon_4 \\ \varepsilon_5 \\ \varepsilon_6 \end{bmatrix} = -\varepsilon_0^2 \begin{bmatrix} \xi_1 \\ \xi_2 \\ \xi_3 \\ \xi_4 \\ 0 \\ 0 \end{bmatrix} u_{\parallel}, \tag{50}$$

For the three cases of orientation of the crystallographic axes in the film, we have

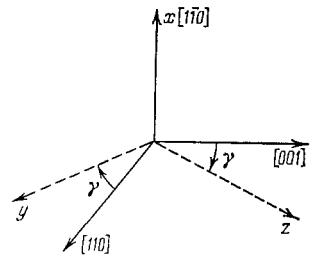

FIG. 6. Rotation of the coordinate system of the waveguide with respect to the crystallographic axes.

a) case 100: $\xi_1 = (2p_{12} - p_{11}h_{100})$;

$$\xi_2 = \xi_3 = p_{11} + p_{12}(1 - h_{100}); \quad \xi_4 = 0; \tag{51}$$

b) case 111: $\xi_1 = 2p_{12} + \frac{2}{3}\Delta p - \left(p_{11} - \frac{2}{3}\Delta p\right) h_{111}$;

$$\xi_2 = \xi_3 = p_{11} + p_{12} - \frac{\Delta p}{3} - \left(p_{12} + \frac{\Delta p}{3}\right) h_{111};$$

$$\xi_4 = 0. \tag{52}$$

c) case 110: $\xi_1 = 2p_{12} + \frac{\Delta p}{2} - \left(p_{11} - \frac{\Delta p}{2}\right) h_{110}$;

$$\xi_2 = p_{11} + p_{12} - \frac{\Delta p}{2} - \left(p_{12} + \frac{\Delta p}{2}\right) h_{110};$$

$$\xi_3 = p_{11} + p_{12}(1 - h_{110}); \quad \xi_4 = 0. \tag{53}$$

We see from (51) and (52) that the film becomes optically uniaxial for the cases 100 and 111 (in case 111 under the additional (46)). In the case 110, as we see from (53), the film is made optically biaxial by the deformation. Hence, by rotating the film with respect to the vertical axis x, one can obtain a nonzero nondiagonal component of the symmetric part of the dielectric-permittivity tensor. For the rotation shown in Fig. 6, we find that in (50) we have

$$\left.\begin{aligned} \xi_2 &= p_{11} + p_{12} - \frac{\Delta p}{2}\cos^2\gamma - \left(p_{12} + \frac{\Delta p}{2}\cos^2\gamma\right) h_{110}, \\ \xi_3 &= p_{11} + p_{12} - \frac{\Delta p}{2}\sin^2\gamma - \left(p_{12} + \frac{\Delta p}{2}\sin^2\gamma\right) h_{110}, \\ \xi_4 &= -\frac{\Delta p}{4}\sin 2\gamma\,(1 + h_{110}) \end{aligned}\right\} \tag{54}$$

(The value of ξ_1 does not change in such a rotation.)

We shall show below that the appearance of a nondiagonal component in the symmetric part of the tensor $\hat{\varepsilon}$ can be employed to obtain nonreciprocal conversion of modes.

Now let us study the magnetooptic anisotropy. Let us introduce the angles defining the direction of magnetization in the system of coordinates associated with the geometry of the waveguide structure (Fig. 7). The direction cosines of the

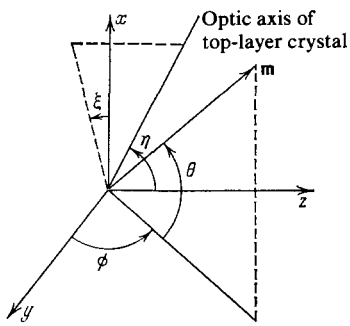

FIG. 7. Angles defining the direction of the magnetization of the film and the optic axis of the top layer.

magnetization will be: $\alpha_1 = \sin\theta$, $\alpha_2 = \cos\theta\cos\phi$, and $\alpha_3 = \cos\theta\sin\phi$. Upon using expressions analogous to (18), (20), and (21), one can derive the following for the three cases of orientation of the film:

a) 100:

$$\begin{bmatrix} \varepsilon_1-\varepsilon_0 \\ \varepsilon_2-\varepsilon_0 \\ \varepsilon_3-\varepsilon_0 \\ \varepsilon_4 \\ \varepsilon_5 \\ \varepsilon_6 \end{bmatrix} = \begin{bmatrix} g_{11}\sin^2\theta + g_{12}\cos^2\theta \\ g_{11}\cos^2\theta\cos^2\phi + g_{12}(\sin^2\theta + \cos^2\theta\sin^2\phi) \\ g_{11}\cos^2\theta\sin^2\phi + g_{12}(\sin^2\theta + \cos^2\theta\cos^2\phi) \\ g_{44}\cos^2\theta\sin 2\phi \\ g_{44}\sin 2\theta\sin\phi \\ g_{44}\sin 2\theta\sin\phi \end{bmatrix} M^2, \tag{55}$$

b) 111:

$$\begin{bmatrix} \varepsilon_1-\varepsilon_0 \\ \varepsilon_2-\varepsilon_0 \\ \varepsilon_3-\varepsilon_0 \\ \varepsilon_4 \\ \varepsilon_5 \\ \varepsilon_6 \end{bmatrix} = \begin{bmatrix} g_{12}+2g_{44}\sin^2\theta+\frac{1}{3}\Delta g \\ g_{12}+2g_{44}\cos^2\theta\cos^2\phi \\ \quad +\frac{1}{3}\Delta g\left(\sin^2\theta+\cos^2\theta\cos^2\phi+\frac{1}{2}\cos^2\theta-\frac{1}{\sqrt{2}}\sin 2\theta\cos\phi\right) \\ g_{12}+2g_{44}\cos^2\theta\sin^2\phi + \\ \quad +\frac{1}{3}\Delta g\left(\sin^2\theta+\cos^2\theta\sin^2\phi+\frac{1}{2}\cos^2\theta+\frac{1}{\sqrt{2}}\sin 2\theta\cos\phi\right) \\ g_{44}\sin 2\phi\cos^2\theta+\frac{1}{6}\Delta g\,(\cos^2\theta\sin 2\phi+\sqrt{2}\sin 2\theta\sin\phi) \\ g_{44}\sin 2\theta\sin\phi+\frac{1}{6}\Delta g\,(2\sin 2\theta\sin\phi+\sqrt{2}\sin 2\phi\cos^2\theta) \\ g_{44}\sin 2\theta\cos\phi+\frac{1}{6}\Delta g\,(2\sin 2\theta\cos\phi-\sqrt{2}\cos 2\phi\cos^2\theta) \end{bmatrix} M^2, \tag{56}$$

c) 110:

$$\begin{bmatrix} \varepsilon_1-\varepsilon_0 \\ \varepsilon_2-\varepsilon_0 \\ \varepsilon_3-\varepsilon_0 \\ \varepsilon_4 \\ \varepsilon_5 \\ \varepsilon_6 \end{bmatrix} = \begin{bmatrix} g_{12}+2g_{44}\sin^2\theta+\frac{1}{2}\Delta g\,(\sin^2\theta+\cos^2\theta\cos^2\varphi) \\ g_{12}+2g_{44}\cos^2\theta\cos^2\varphi+\frac{1}{2}\Delta g\,(\sin^2\theta+\cos^2\theta\cos^2\varphi) \\ g_{12}+2g_{44}\cos^2\theta\sin^2\varphi+\Delta g\cos^2\theta\sin^2\varphi \\ g_{44}\cos^2\theta\sin 2\varphi \\ g_{44}\sin\varphi\sin 2\theta \\ \left(g_{44}+\frac{\Delta g}{2}\right)\sin 2\theta\cos\varphi \end{bmatrix} M^2, \tag{57}$$

d) upon rotation the crystal about the x axis (see Fig. 6)

$$\begin{bmatrix} \varepsilon_1-\varepsilon_0 \\ \varepsilon_2-\varepsilon_0 \\ \varepsilon_3-\varepsilon_0 \\ \varepsilon_4 \\ \varepsilon_5 \\ \varepsilon_6 \end{bmatrix} = \begin{bmatrix} g_{12}+2g_{44}\sin^2\theta+\frac{\Delta g}{2}[\sin^2\theta+\cos^2\theta\cos^2(\phi-\gamma)] \\ g_{12}+2g_{44}\cos^2\theta\cos^2\phi+\frac{\Delta g}{2}\left\{\sin^2\theta\cos^2\gamma\right. \\ \quad \left.+\frac{1}{2}\cos^2\theta\left[\frac{3}{2}\sin^2 2\gamma+\cos\phi\cos(\phi-2\gamma)(3\cos^2 2\gamma-1)\right]\right\} \\ g_{12}+2g_{44}\cos^2\theta\sin^2\phi+\frac{\Delta g}{2}\left\{\sin^2\theta\sin^2\gamma\right. \\ \quad \left.+\frac{1}{2}\cos^2\theta\left[\frac{3}{2}\sin^2 2\gamma+\sin\phi\sin(\phi-2\gamma)(3\cos^2 2\gamma+1)\right]\right\} \\ g_{44}\cos^2\theta\sin 2\phi+\frac{\Delta g}{4}\sin 2\gamma\{1-3\cos^2\theta[\cos^2\gamma-\cos\phi\cos(\phi \\ -2\gamma)]\} \\ g_{44}\sin\phi\sin 2\theta+\frac{\Delta g}{2}\sin\gamma\sin 2\theta\cos(\phi-\gamma) \\ g_{44}\cos\phi\sin 2\theta+\frac{\Delta g}{2}\sin 2\theta\cos\gamma\cos(\phi-\gamma) \end{bmatrix} M^2. \tag{58}$$

In principle one can write analogous expressions also for the tensor $\hat{\mu}$.

Upon taking into account the approximation (22), we obtain the following expressions for the components of the antisymmetric part of the tensors $\hat{\varepsilon}$ and $\hat{\mu}$:

$$a_1 = f^{\varepsilon}M\sin\theta,\quad a_2 = f^{\varepsilon}M\cos\theta\cos\phi,\quad a_3 = f^{\varepsilon}M\cos\theta\sin\phi \tag{59}$$

and analogous expressions for b_i, e.g., $b_1 = f^{\mu}M\sin\theta$.

One can analyze a concrete situation on the basis of Eqs. (36) and (45) and the concrete form of the tensors $\hat{\varepsilon}$ and $\hat{\mu}$. As an example, let us study an undeformed ($u_{\parallel} = 0$) film of a ferrite garnet on a nonmagnetic {111} substrate (the top layer is air).

By using (56), (59), and (45), we find that

$$\varepsilon_0 \operatorname{Re} k^{\pm} = -B^f g_{44} M^2 \sin 2\phi \cos^2\theta \mp A^f \beta_h^0 f^e M \cos\theta \sin\phi,$$
$$\varepsilon_0 \operatorname{Im} k^{\pm} = \beta_h^0 A^f g_{44} M^2 \sin 2\theta \cos\phi \pm B^f f^e M \sin\theta. \quad (60)$$

For simplicity we have omitted the terms pertaining to the tensor $\hat{\mu}$; we have assumed the quadratic magnetooptic contribution to the dielectric permittivity to be isotropic ($\Delta g = 0$), and we have introduced the notation

$$A^f \equiv \langle \mathscr{H}\mathscr{E} \rangle^f, \quad B^f = \left\langle \mathscr{E} \frac{d\mathscr{H}}{dx} \right\rangle^f. \quad (61)$$

The superscript f indicates that the integration is performed within the limits of the film. If we select $\phi = 0$ and take the parameters of the film such that the following relationship holds:

$$\cos\theta = B^f f^e / 2\beta_h^0 A^f g_{44} M \quad (62)$$

then we find that

$$k^+ = 0, \quad \text{a} \quad k^- = i2B^f f^e M \sin\theta \cdot \varepsilon_0^{-1}. \quad (63)$$

Thus there is no conversion for the forward wave, while it exists for the backward wave.

If we choose the Faraday geometry ($\theta = 0$, $\phi = \pi/2$), then we find from (60) that

$$k^{\pm} = \mp A^f \beta_h^0 f^e M \varepsilon_0^{-1}. \quad (64)$$

That is, nonreciprocity is lacking in this geometry ($|k^+| = |k^-|$).

According to (43), the propagation length that corresponds to the maximal conversion under the condition of mode synchronization ($\Delta' = 0$) is increased in the case of (63) as compared with the Faraday geometry by a factor of $A^f / B^f \sin\theta$. From the standpoint of decreasing the length l, one must choose a film thickness close to the region of cutoff of the modes where the quantity B^f has a maximum. However, the mismatch Δ^0 also has a maximum in this region (see Fig. 2) that is difficult to compensate (see Sec. 3) with the anisotropy of the epitaxial film.

As the second example, let us study a film grown on the {110} plane. By using (54), (58), and (45), we can find that we have the following expression instead of (64) for the Faraday geometry in the given case under the same assumptions:

$$k^{\pm} = -[\varepsilon_0 \Delta p (1 + h_{110}) u_{\parallel}] \left(\frac{\sin 2\gamma}{4}\right) B^f \pm f^e M \varepsilon_0^{-1} A^f. \quad (65)$$

That is, it proves possible in this case to obtain nonreciprocity of the coupling coefficient in the Faraday geometry.

As yet another possibility of obtaining nonreciprocal conversion, let us study a film made of a gyrotropic material and a top layer made of an anisotropic material.[32,48-50] We obtain from (45) that the condition $|k^+| = 0$ requires us to have

$$\varepsilon_4^t B^t = -a_3^f \beta_h^0 A^f, \quad \beta_h^0 \varepsilon_6^t A^t = -a_1^f B^f. \quad (66)$$

For simplicity we have omitted the terms containing components of $\hat{\mu}$.

As the top layer, let us study an optically uniaxial crystal, the direction of whose optic axis is defined by the angles η and ζ (Fig. 7). The components of the dielectric-permittivity tensor will have the form

$$\begin{bmatrix} \varepsilon_1^t - \varepsilon^0 \\ \varepsilon_2^t - \varepsilon^0 \\ \varepsilon_3^t - \varepsilon^0 \\ \varepsilon_4^t \\ \varepsilon_5^t \\ \varepsilon_6^t \end{bmatrix} = \begin{bmatrix} \cos^2\zeta \cdot \sin^2\eta \\ \sin^2\zeta \cdot \sin^2\eta \\ \cos^2\eta \\ \frac{1}{2}\sin\zeta \cdot \sin 2\eta \\ \frac{1}{2}\cos\zeta \cdot \sin 2\eta \\ \frac{1}{2}\sin 2\zeta \cdot \sin^2\eta \end{bmatrix} \cdot \Delta\varepsilon. \quad (67)$$

Here we have $\Delta\varepsilon = \varepsilon^e - \varepsilon^0$, while ε^e and ε^0 are respectively the squares of the refractive indices of the extraordinary and ordinary rays of the top-layer crystal. As we see from (67), the maximum of the quantity ε_4^t corresponds to the direction of the optic axis: $\eta = \pi/4$ and $\zeta = \pi/2$. Here we see from (67) that $\varepsilon_6^t = 0$. Thus, in the Faraday geometry for which $a_1^f = 0$, the second equation of (66) is fulfilled. An anisotropic top layer can be used at the same time to attain phase synchronization of the modes ($\Delta^0 = \delta_h - \delta_e$). When $\zeta = \pi/2$, we find that $\delta_h^t \simeq 0$. In order to have $\delta_e < 0$, as (36) implies, we must use a negative crystal as the top layer ($\varepsilon^0 > \varepsilon^e$). The experimental studies of nonreciprocity in structures with anisotropic top layers will be described in Sec. 4. Here we note only that the practical application of epitaxial films of ferrite garnets without anisotropic top layers, encounters difficulties in connection with the large mismatch in the cutoff region. The investigation of anisotropic top layers leads to an appreciable technical complication of the instrumentation (see Sec. 4).

One of the possible variants of the solution of the problem is to use periodic magnetic waveguides[51-54] in which phase matching of the interacting modes occurs periodically, rather than matching of their phase velocities, as in the case of anisotropic structures.

Usually one analyzes such periodic structures on the basis of the transfer matrix,[55] which can be derived from solving Eq. (40) for the coupled modes. This matrix (T) relates the amplitudes of the fields at the beginning ($z \equiv z_0$) and at the end (z) of propagation:

$$\begin{bmatrix} e(z) \\ h(z) \end{bmatrix} = e^{-i\bar{\beta}(z-z_0)} \begin{bmatrix} T_{11} & T_{12} \\ T_{21} & T_{22} \end{bmatrix} \begin{bmatrix} e(z_0) \\ h(z_0) \end{bmatrix}. \quad (68)$$

Here we have

$$T_{11} = \cos\nu(z - z_0) + \frac{i\Delta'}{2\nu}\sin\nu(z - z_0),$$
$$T_{12} = \frac{k}{\nu}\sin\nu(z - z_0),$$
$$T_{21} = -\frac{k^*}{\nu}\sin\nu(z - z_0),$$
$$T_{22} = \cos\nu(z - z_0) - \frac{i\Delta'}{2\nu}\sin\nu(z - z_0).$$

Here the matrix T is written for a region of the waveguide having a homogeneous distribution of the magnetization. For a waveguide with a periodic magnetic structure, one can derive the conversion matrix by multiplying the conversion matrices for the individual "homogeneous" regions. For ex-

ample, in the case of periodic variation of the direction of magnetization along the z axis with the period $z-z_0 = \pi/\nu$, one can easily find that the conversion coefficient will be determined by the expression

$$R = \sin^2 2p \arcsin \frac{|k|}{\nu}, \tag{69}$$

Here p is the number of periods. Hence we see that one can obtain $R = 1$ by an appropriate choice of the number of periods. The total length of the structure in real units will be

$$l = \frac{p\lambda}{2\nu}. \tag{70}$$

One can also analyze other "cascade" structures by using the matrix (68), including nonreciprocal ones (see Sec. 4).

In order to build nonreciprocal devices, one can use waveguides of the "semileaky type" of (32). One of the possible variants of an isolator based on such a waveguide has been studied in Ref. 50 (see Sec. 4). Along this line, it is of interest to study the conversion between guided and radiative modes.[42-44] Let us study the case in which the TE mode is the guided mode and the TM mode is the "leaky" mode (see (32)). Figure 8 shows the situation corresponding to the case in which the material of the substrate and of the film are isotropic, while the anisotropy of the top layer is such that $\varepsilon_1^t > \varepsilon^f > \varepsilon_2^t$. Then the normal modes of TE polarization will include guided modes having discrete eigenvalues β, while those with TM polarization will consist of radiative modes with a continuous spectrum (damped modes corresponding to imaginary values of β play no substantial role below, and we shall not treat them). We see from the diagram that the discrete spectrum of TE modes overlaps the continuous spectrum of TM modes belonging to both the film and the top layer. The diagram shows the profiles of the fields in different regions of the spectrum of modes. The radiative modes belonging to the film and the top layer have a sinusoidal field distribution, both in the film and in the top layer, and they decay exponentially in the substrate.

Thus, in contrast to the case of interaction between guided modes, the condition of phase matching is always satisfied in the interaction of guided modes with radiative modes. Instead of (41), we have the following expression in this case for the conversion coefficient[43]:

$$R(z) = 1 - \exp(-2\alpha z). \tag{71}$$

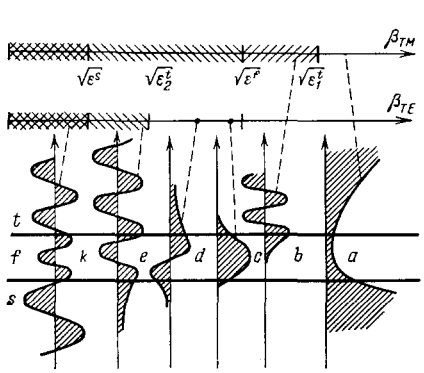

FIG. 8. Distribution of fields: a) not realizable; b)modes of the top layer; c and d) guided modes; e) "film-top layer" radiative modes; k) "film-top layer-substrate" radiative modes.

Here the decay constant α arising from coupling of the guided mode with the radiative modes is determined by the expression

$$\alpha = \frac{\pi\varepsilon_3^t}{\varepsilon_1^t}\left[|k(\beta)|^2 \frac{\beta\sqrt{\varepsilon_1^t}}{\sqrt{\varepsilon_2^t}\sqrt{\varepsilon_1^t-\beta^2}}\right]_{\beta=\beta_g}. \tag{72}$$

Here β_g is the effective refractive index of the guided $\beta = \beta_g$ mode, while the coupling coefficient k for the case in which only the components a_3^f and ε_4^t of the dielectric-permittivity tensor differ from zero is given by the expression

$$\operatorname{Re} k^{\pm} = \frac{\omega}{4p}\left(\pm\int_{-d/2}^{d/2} a_3^f \mathscr{E}^g \mathscr{H}^r\, dx + \int_{d/2}^{\infty} \varepsilon_4^t \mathscr{E}^g \frac{d\mathscr{H}^r}{i dx}\, dx\right). \tag{73}$$

At the same time, we have $\operatorname{Im} k^{\pm} = 0$ (since $\varepsilon_6 = a_1 = 0$). Here the superscripts "g" and "r" respectively pertain to the guided and radiative modes, while p is a normalizing constant having the dimensions of power.

Thus here, just as in the case of interaction of guided modes, one can obtain nonreciprocity of the coupling coefficient by an appropriate choice of the quantities a_1^f and ε_4^t to make the integrals in (73) identical in magnitude. If, for example, we have $k^+ = 0$, $k^- \to \infty$, then the structure will behave as an isolator that transmits the TE wave in the forward direction without transmitting waves of either TE or TM polarization in the backward direction. In contrast to an isolator based on interaction of guided modes, this isolator requires no mode filter (see Sec. 4), since the radiative modes are conducted (leak) out of the waveguide.

Let us examine the requirements imposed on such a structure in order that the integrals in (73) should have as large values as possible while identical in magnitude. As regards the first integral in (73), to increase it one must use a film made of an isotropic material. Then the transverse wave number of the TE guided mode $k_0\gamma_g = k_0\sqrt{\varepsilon_2^f - \beta_g^2}$ will be equal to the transverse waveguide number of the TM "film-top layer" radiative mode $k_0\gamma_r = k_0\sqrt{\varepsilon_3^f/\varepsilon_1^f}\sqrt{\varepsilon_1^f - \beta_r^2}$ while the longitudinal waveguide numbers are equal: $k_0\beta_r = \beta_g k_0$. Here the overlap integral will have a maximum value.

As we see from Fig. 8, the guided mode and the "film-top layer" radiative mode have substantially different variations in the overlap region. Nevertheless, as calculation shows,[43] the second integral in (73) can have a maximum near $\beta_r = \beta_g$, independently of the thickness of the film, of a magnitude that makes the two integrals in (73) comparable in value.

The imaginary component of the coupling coefficient arising from the components of the dielectric-permittivity tensor ε_6^t and a_1^f has an infinitesimally small term containing the component ε_6^t of the tensor at $\beta_r = \beta_g$, in contrast to the case of interaction of guided modes. Thus the variant of the nonreciprocal mode converter employing the imaginary component of the coupling coefficient fails in the case of interaction of a guided mode with a radiative mode. Section 4 will study a concrete waveguide structure employing the interaction of a guided TE mode with radiative modes for design of an optical valve.

It is of especial interest to study the waveguide propagation of light in four-layer waveguides and those with more

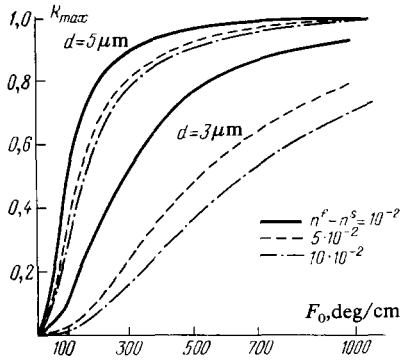

FIG. 9. Dependence of the $TE_0 \rightleftarrows TM_0$ conversion for the optimal propagation distance on the specific Faraday rotation for two film thicknesses and three refractive indices of the substrate for $n^f = 2.2$, $\lambda = 1.15\ \mu m$.[53]

layers. The point is that real epitaxial films are often layered (see Sec. 3). Then their waveguide properties can be described by the model of a multilayer waveguide. Moreover, in such heterostructures one can obtain the waveguide properties necessary in practice (see Sec. 3). For example, in such structures one can obtain synchronization near the mode cutoff.[56-57]

The dispersion equations for a four-layer isotropic structure have been derived in Ref. 59. Figure 9 shows the dependences of $R_{max} = (|k|/\nu)^2$ calculated for the fundamental modes on the specific Faraday rotation in the case in which the refractive index of the film is close to that of the substrate. We see from the diagram that one can increase the conversion with a constant Faraday rotation by decreasing the difference $n_f - n_s$. For example, for $d = 3\ \mu m$, $n_f - n_s = 10^{-2}$, and $F_0 = 300\,d$ deg/cm, we find from Fig. 9 that $R_{max} = 0.5$, whereas for an analogous structure, but with $n_f - n_s = 0.3$, one can calculate that $R_{max} = 0.15$. Thus, by using an intermediate film one can increase the mode conversion, including the region near cutoff.

3. EPITAXIAL FILMS OF FERRITES HAVING THE GARNET STRUCTURE—OPTICAL WAVEGUIDES

Polycrystalline films of the ferrite garnets have been proposed as a magnetooptical medium for designing various functional elements of integrated optics.[59] The technology of growing such films has been developed in connection with application in memory devices based on cylindrical magnetic domains. Moreover, they can find widespread application in UHF technology employing spin waves. As we shall show in Sec. 4, these films can also find application in various functional elements of integrated optics.

In this section we shall briefly treat the properties of epitaxial films of ferrite garnets that govern their waveguide characteristics, and also discuss the studies that have treated the properties of epitaxial garnet films by the waveguide method.

First let us take up the mechanical properties of these films. The stresses and strains existing in epitaxial films can affect their magnetic and optical properties, owing to magnetostriction and photoelasticity. In this regard, it seems important to take up, however, briefly, the stresses in epitaxial films.

The nature of the stresses in them involves the fundamental question of epitaxy—the character of the matching of the crystal lattices of the film and the substrate (see, e.g., Ref. 60). The studies of epitaxial films of ferrite garnets[61-70] have shown that their stressed state is described rather well by the accommodation model proposed in Ref. 67. According to this model, one can distinguish two regions of the stressed state of the film, depending on the magnitude of the mismatch.

$$f = \frac{a_s - a_0}{a_0}. \tag{74}$$

Here a_0 is the lattice parameter of a massive specimen of the film material at room temperature, and a_s is the lattice parameter of the substrate at room temperature. At sufficiently low values of $f(\sim 10^{-3})$, the epitaxial film deforms elastically until its lattice paramter along the phase boundary equals that of the substrate (region of surface pseudomorphism). At larger values of f, complete match of parameters does not occur, and certain atomic layers in the film (or in the substrate) do not continue into the substrate (or film)—dislocation mismatch arises. Thus, at the temperature of growth of the film with large mismatches of parameters, a fraction of the elastic stress of the region of pseudomorphism appears to be relieved by formation of mismatch dislocations. Thus the final planar deformation $u_{||}$ of the film is determined by the expression

$$u_{||} = f - \delta, \tag{75}$$

Here $\delta = (a_s - a_{f||})/a_0$ is the accommodation of the film arising from formation of mismatch dislocations, we have $u_{||} = (a_{f||} - a_0)/a_0$, and $a_{f||}$ is the lattice parameter of the film along the phase boundary.

One can derive the following expression[63,65] for the magnitude of the elastic deforation of the film at room temperature:

$$u_{||} = f(1 - \eta) + \Delta\alpha \cdot \Delta T \eta, \tag{76}$$

Here $\Delta\alpha = \alpha_f - \alpha_s$ is the difference in temperature coefficients of linear exansion of the materials of the film and the substrate, ΔT is the difference between the growth temperature and room temperature, and the annealing parameter is

$$\eta = \frac{b_{f||} - b_s}{b_0 - b_s}. \tag{77}$$

Here the b_i are the corresponding lattice parameters at the temperature of growth of the film. The expression (77) is valid if we assume that no additional annealing of the film occurs upon cooling. In the converse case, η in (76) must characterize the total accommodation (both at the time of growth and during cooling). In the pseudomorphism region ($\eta = 0$), complete match of the lattice parameters of the film and the substrate at the phase boundary occurs, while when $\eta = 1$, the stresses at the temperature of growth are fully relieved by formation of mismatch dislocations. There is a smooth transition between these regions when the stresses are partially relieved by mismatch dislocations. This transition region has been found experimentally in Ref. 65.

In Ref. 67 a study was made of the process of formation of mismatch dislocations by bending them and extending them along the phase boundary of the film and the substrate. As a result this study obtained the time- and temperature-dependence of the annealing parameter, which has been discussed for the garnets in Refs. 63 and 64. Qualitatively the model describes the experimental data,[65] although, owing to lack of the latter, one cannot at present speak of quantitative agreement.[64]

As is evident from Sec. 2, it is important in waveguide magnetooptics to obtain phase synchronization near the cutoff of the modes. To do this, as will be shown below, one needs epitaxial films with deformations exceeding 10^{-2} (another possibility is two-layer films). In this regard the question arises of the possibility of growing films with such deformations. As is known, at mismatches $|f| > 1.5\text{–}3\times10^{-2}$, even nucleation of the film crystal ceases,[68–69] while the region of pseudomorphism is restricted to values $|f| \sim 2\times10^{-3}$. Outside this region, the quality of the films usually deteriorates.[64,66,68]

According to Ref. 71, the magnitude of the linear expansion coefficient for the garnets depends weakly on substitution in the dodecahedral lattice sites. For the aluminates, gallates, and ferrites, it amounts respectively to 8.6×10^{-6}, 9.2×10^{-6}, and 10.4×10^{-6} K^{-1}. At growth temperatures $\sim10^3$ K, the quantity $\Delta\alpha\cdot\Delta T$ is $\sim2\times10^{-3}$, and it determines the deformation in the regions when $\eta\approx1$. Thus one should seek an increase in the strain in garnet films by way of extending the region of pseudomorphism, which, however, is unlikely.[64]

At large tensile strains, cracking of the films can occur. For a brittle material such as garnet one can estimate the critical value of f by the formula[72]

$$f_{cr}^{A} = (1-\nu)\sqrt{\frac{c}{5\pi d}}. \tag{78}$$

Here ν is the Poisson coefficient (see below, Table I), c is the interatomic distance (~3Å), and d is the thickness of the film. Here we have assumed that $\eta = 0$. A mismatch of lattice parameters exceeding f_{cr}^{A} is a necessary, but not yet a sufficient condition for formation of cracks. If the film contains no centers for crack formation, then fulfillment of the condition $f > f_{cr}^{A}$ does not lead to cracking. Spontaneous crack formation will occur if[72]

$$f > f_{cr}^{B} = \frac{1-\nu}{10}. \tag{79}$$

Figure 10 shows the predictions of Eqs. (78) and (79). If the parameters of the film correspond to points under the line 1, then a crack will not propagate, even if the film contains centers of crack formation; between the lines 1 and 2, crack

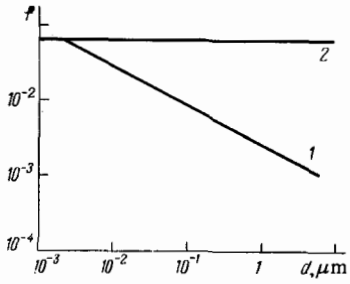

FIG. 10. Diagram of the mechanical state of an epitaxial film.[72]

formation requires the existence of centers (scratches, inclusions, etc.); above the line 2 cracks will form spontaneously. Thus in theory, one can obtain films with a mismatch 10^{-3}–10^{-2} and of thickness 1–10 μm, as are usually employed in waveguide optics, without cracking if they contain no defects that could serve as centers for crack formation. What we have said above pertains to stretched films. In waveguide magnetooptics, more often films in the compressed state are used. Under the condition $\eta = 0$, such films contain no cracks.[61] However, when a certain critical film thickness and magnitude of mismatch are exceeded, they can exfoliate from their substrate and then crack. Other possible mechanisms of crack formation are: breakdown of the substrate itself along planes perpendicular to the film,[72] or shear stresses caused by screw dislocations.[64]

Table I gives the values of the stiffness constants, the Poisson coefficient, and parameters h_{111} for certain garnets according to Ref. 73.

The garnets resemble an elastically isotropic material ($\Delta c = 0$) in their elastic properties. As we have already noted, the elastic properties of epitaxial garnet films affect the most important characteristics of light propagating in waveguide fashion (see Sec. 2). Therefore a knowledge of these properties and ability to control them by ion substitution in the garnet lattice define in many ways the possible application of these films in integrated and waveguide optics.

The magnetic properties of epitaxial films of ferrite garnets have been widely discussed in connection with the problem of cylindrical magnetic domains. Hence we shall take them up here very briefly. The equilibrium direction of spontaneous magnetization of a monocrystalline film of a ferrite is determined by the minimum of the magnetic energy:

$$E = E_c + E_\sigma + E_G + E_H + E_D. \tag{80}$$

The energy of the crystallographic cubic anisotropy is

$$E_c = K_1(\alpha_1^2\alpha_2^2 + \alpha_1^2\alpha_3^2 + \alpha_2^2\alpha_3^2) + \ldots. \tag{81}$$

Here K_1 is the first cubic anisotropy constant, and the α_i are

TABLE I.

Composition	C_{11}	C_{12}	C_{44}	ΔC	$\nu = \frac{C_{12}}{C_{11}+C_{12}}$	h_{111}
	10^{11} dyne/cm^2					
$Y_3Fe_5O_{12}$	26,8	11,06	7,66	0,42	0,292	0,85
$Y_3Ga_5O_{12}$	29,03	11,73	9,547	−1,794	0,288	0,74
$Y_3Al_5O_{12}$	33,32	11,07	11,5	−0,75	0,249	0,64
$Eu_3Fe_5O_{12}$	25,10	10,70	7,62	−0,84	0,299	0,81

the direction cosines of the magnetization with respect to the fourfold axes. If we assume that (46) holds, the energy involved in the stresses in the film[74] has the form

$$E_\sigma = \left[\frac{3}{2}\lambda_{100}\left(\alpha_1^2\beta_1^2+\alpha_2^2\beta_2^2+\alpha_3^2\beta_3^2-\frac{1}{3}\right)\right.$$
$$\left.+3\lambda_{111}\left(\alpha_1\alpha_2\beta_1\beta_2+\alpha_2\alpha_3\beta_2\beta_3+\alpha_1\alpha_3\beta_1\beta_3\right)\right]\sigma_\parallel. \quad (82)$$

Here $\sigma_\parallel$ is the in-plane stress, the λ_i are the magnetostrictive constants along the corresponding axes, and the β are the direction cosines of the normal to the film with respect to the cubic axes. The energy of growth anisotropy[74] is expressed in terms of the constants A and B:

$$E_G = A\left(\alpha_1^2\beta_1^2+\alpha_2^2\beta_2^2+\alpha_3^2\beta_3^2-\frac{1}{3}\right)$$
$$+B\left(\alpha_1\alpha_2\beta_1\beta_2+\alpha_2\alpha_3\beta_2\beta_3+\alpha_1\alpha_3\beta_1\beta_3\right). \quad (83)$$

The energy of interaction with the external field is

$$E_H = -\mathbf{MH}. \quad (84)$$

The energy of demagnetization for the case of a homogeneously magnetized film is

$$E_D = 2\pi M^2\left(\alpha_1\beta_1+\alpha_2\beta_2+\alpha_3\beta_3\right)^2 = 2\pi M^2\cos^2\xi. \quad (85)$$

Here ξ is the angle between the magnetization direction and the normal to the plane of the film.

Periodic magnetic structures may be of interest for waveguide and integrated optics, either when created in the film by an external field, or inherent in the film itself.[29,51–54] The parameters of stripe domains are determined by the minimum of the energy of the domain walls and the demagnetization[72]:

$$E = \frac{2W}{D}+8M^2\frac{D\cos^2\xi}{\pi^2 d}\sum_{n=1,3,5,\ldots}^{\infty}\left[1-\exp\left(-\frac{2\pi nd}{D}\right)\right]. \quad (86)$$

Here W is the wall energy density per unit surface, and D is the period of the stripe domain structure. The second term in (86) has been derived under the assumption that the wall thickness is small in comparison with the period of the structure. For a homogeneously magnetized film ($D\to\infty$), Eq. (86) reduces to (85). In the garnets the period of the stripe domains lies in the range 1–25 μm. These structures can be used to design matching elements and mode converters. Section 4 will treat the problem of using periodic magnetic structures in integrated optics using concrete examples (see also Ref. 29).

The domain structure realized in the film is determined by the energy minimum in (80) and (86). Depending on the relationship of the different contributions to the overall energy, both period and irregular structures can be realized. In addition to the films with stripe domains noted above, films are of interest in which the magnetization lies in a plane ("easy-plane" type), and according to (85), the demagnetizing field is zero. With a small coercive force and anisotropy in the plane of the film, one can control the magnetization with very small fields (~0.1 Oe). Usually such films have broad domains, which can be observed by ordinary methodology in polarized light by placing the film at 45° to the optic axis of the microscope.[52] If the total energy in (80) is mainly governed by the contribution E_σ associated with stresses, then films grown on {111} substrates will have the corresponding energy.

$$E_\sigma = -\frac{3}{2}\sigma_\parallel\lambda_{111}\cos^2\theta. \quad (87)$$

Thus the magntization will lie in the plane of the film ($\theta=0$) for ferrites with $\lambda_{111}<0$ in the case of films in the compressed state ($f<0$). Since yttrium iron garnet has a lattice parameter smaller than gadolinium gallium garnet (GGG), then when one uses the latter as the substrate, one must replace iron and/or yttrium ions with those of larger dimension, e.g., scandium and gadolinium ions, respectively. One must study the problem of the choice of replacement jointly with the magnetooptic, optical, and other properties.[75] Certain compositions useful for application in integrated optics have been given in Ref. 76. A defect of the garnets of the scandium system is small values of the factor $M_1=(F_0/4\pi M_s)^2<0.14$ (deg/cm·G)^2. In the gadolinium system M_1 is larger and reaches 11.7 (deg/cm·G)^2. Introduction of Pr^{3+} ions leads to very large negative values of the Faraday rotation constants.[26a,77] Introduction of Pr^{3+} ions together with Bi^{3+} and Yb^{3+} ions made possible obtaining films with an anisotropy of the "easy-plane" type and a large negative Faraday rotation.[76] Certain parameters of films of this system are given in Table II (data taken from Ref. 76). Here α is the attenuation constant, and F_0 is the Faraday rotation constant. An important characteristic of the garnets for waveguide magnetooptics is the refractive indices. Their approximate values for the ferrites (~2.22), gallates (~1.95), and aluminates (~1.85) have been given in Ref. 59. Since the refractive indices of the garnets mainly arise from absorption bands in the visible and ultraviolet regions of the spectrum, in the near infrared one observes only a weak dispersion of the refractive index. Moreover, n varies somewhat with different replacements in the rare-earth sublattice. In particular, compositions containing ions of large radius (such as Bi^{3+} and Pr^{3+}) have larger values of n.

TABLE II.

Composition	a_s-a_0, Å	$4\pi M_s$, Gauss	F_0, deg/cm	M_1, (deg/cm·G)^2	$M_2\equiv F_0/\alpha$, deg/dB	
$(Yb, Pr)_{2,5}Bi_{0,5}Fe_4Ga_1O_{12}$	−0,031	270	−675	6,25	160	$n=2,25$ $\lambda=1,15$ μm
$(Yb, Pr)_{2,3}Bi_{0,7}Fe_{3,8}Ga_{1,2}O_{12}$	−0,002	150	−950	40		
$(Yb, Pr)_{2,1}Bi_{0,9}Fe_{3,85}Ga_{1,15}O_{12}$	−0,019	220	−1190	30		

Investigation of waveguide propagation of light consists of studying the spectrum of modes (dependence of the light intensity on the value of β), and effects of conversion and absorption dispersion. Here one can determine the refractive index, the thickness, the birefringence, and Faraday and Voigt constants,and the magnitude of the absorption and scattering. From the standpoint of using the films in integrated optics, the important characteristics of a film are the maximum amount of conversion, the minimum distance corresponding to this conversion, and nonreciprocity of conversion. The magnitude of the coupling coefficient and the mismatch are also of interest.

Different mthods of studying waveguide propagation of light in thin films have been described in a number of original and review studies (see, e.g., Refs. 5–7). The possibilities of this method of studying the properties of thin films are still far from being exhausted. Since we can not take time to discuss the method, we refer the reader to the literature cited in Refs. 5–7, 78, and 79.

Let us examine what information one can obtain from measuring the values of β_m. As is known,[5–7] the accuracy of determining β_m, for example by the method of prism input, amounts to 10^{-4}–10^{-5}. The sum of the deviations in the least-squares method is

$$\sigma=\frac{1}{k}\sum_{m=0}^{k-1}[\tilde{\beta}_m-\beta_m(n,\ d)]^2. \tag{88}$$

Here the β_m are the experimental values of the effective refractive index of the mth-order mode, and the B_m are the calculated values for an isotropic waveguide with an ideal refractive-index step profile, and k is the number of the modes. The magnitude of σ for modes of the same polarization evidently must not exceed 10^{-8}–10^{-10}. In this case n and d are determined with an accuracy of respectively 10^{-4}–10^{-5} and 10^{-3}.[5–7]

As a rule, real epitaxial films of ferrite garnets do not possess an ideal step profile of the refractive index, owing to existence of transition boundary layers[80] or inhomogeneities throughout the thickness of the film.[81–82] One should also take into account the existence of birefringence (see below) and of the air gap between the prism and the film.[79]

When the value of σ exceeds the value arising from experimental error, in an isotropic structure this implies a deviation of the refractive-index profile from the ideal. Usually here the distortions in the case of inhomogeneities in the bulk of the film differ from the distortions that arise from existence of transition boundary layers. Namely, in the former case the entire spectrum is distorted, while boundary layers exert a stronger influence on the higher-order modes. This involves the differing energy distribution of the modes through the thickness of the film for modes of different orders. Unfortunately, the effect of different inhomogeneities in epitaxial films on the mode spectrum has not been studied broadly enough, As a rule, in the studies on the mode spectrum in epitaxial garnet films, the value of σ is not indicated. Hence one cannot estimate the accuracy of the values of the parameters derived from the mode spectrum. In addition, measurement of the distortion of the mode spectrum characterizes the inhomogeneity of the films, which sometimes cannot be found by other methods.

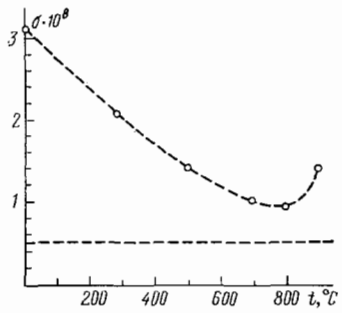

FIG. 11. Variation of the quadratic deviation of the spectrum of TE modes upon annealing an epitaxial garnet film.[81]

Reference 81 has studied the effect of annealing on the magnitude of the distortion of the mode spectrum (σ). It was determined from the nature of the distortions that the latter are associated not with boundary layers, but with the layered nature of the films throughout the thickness. Figure 11 shows the dependence of σ on the temperature of annealing, which was carried out for two hours at each point. We see that the homogeneity of the films increases with increasing annealing temperature. Apparently the increase in σ at temperatures about 900 °C involves blurring of the film-substrate boundary by diffusion of ions across the boundary.

One can determine the linear birefringence in films by measuring either the spectrum or the mode conversion. In the former case, for thick enough films in which more than two modes of each polarization can propagate, one determines the value of ε_2 by measuring the specturm of the TE modes, and ε_1 by measuring the TM modes. Here the error of measuring the birefringence amounts to $6\times10^{-4}/\sqrt{k}$, where k is the number of modes in the film.[83]

By using (36) one can find that the birefringence Δn for modes far from cutoff is determined by the approximate expression[83]

$$\Delta n\equiv\sqrt{\varepsilon_1}-\sqrt{\varepsilon_2}\approx\Delta^0-\Delta'. \tag{89}$$

It was assumed in deriving this expression that all the energy of the modes is concentrated in the film and that $B^0_e\approx\beta^0_h\approx\sqrt{\varepsilon_0}$.

The magnitude of the mismatch Δ' can be found in absolute value by measuring the conversion as a function of the propagation distance. One can also determine from these measurements the mode-coupling coefficient. By using (41) one can find that

$$|\Delta'|=\frac{\lambda\sqrt{1-R_{\max}}}{2l_0},\quad |k|=\frac{\lambda\sqrt{R_{\max}}}{4l_0}. \tag{90}$$

Here l_0 is the propagation distance of the light corresponding to the maximum conversion coefficient. We note that one can determine Δ' only in absolute value by measuring mode conversion, since the mismatch enters (41) only as the square. Moreover, one can find Δ' from measuring $R(z)$ only if one can obtain a curve with a maximum, which is difficult in the case of films with a large Faraday rotation, for which $l_0\sim1$ mm, as well as strongly absorbing films. It is impossi-

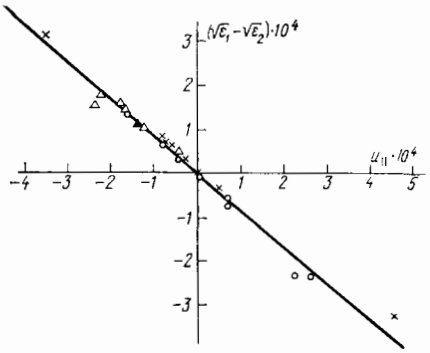

FIG. 12. Dependence of the birefringence on the deformation of epitaxial films of YTbFeAl and YGdFeGa from Refs. 38 (triangles); 84, 87 (crosses); 45, 86 (dots).

ble if the dimension of the film is less than l_0. In all these cases, and also if one must know the sign of the mismatch, one must employ measurements of the mode spectrum.

Experimental studies of birefringence in films have been carried out in Refs. 38 and 83–87. The deformation of an epitaxial film was determined there by x-ray measurements, while the birefringence was found from waveguide measurements. Figure 12 shows the dependence of the birefringence on the deformation as derived from the experimental data of Refs. 38, 84, and 86, which studied films of the YTbFeAl and YGdFeGa systems. A linear $\Delta n(u_{\parallel})$ relationship was found within the limits of experimental error. This implies that the photoelasticity constants p_{44} are independent of the composition in these films. Upon employing (50), one can find that

$$p_{44}=\frac{\sqrt{\varepsilon_1}-\sqrt{\varepsilon_2}}{n_0^3(u_{\parallel}-u_{\perp})}=\frac{\sqrt{\varepsilon_1}-\sqrt{\varepsilon_2}}{n_0^3(1+h_{111})u_{\parallel}}. \quad (91)$$

One can find the mean value, $\bar{p}_{44}=-0.045\pm 0.005$ from the data of Refs. 38, 84, and 86. This agrees with the data found[23] for a series of garnets from measuring the birefringence under uniaxial compression (the positive sign of the constant in Ref. 23 is in error). Table III gives the characteristics of epitaxial films from Refs. 38, 84, and 86. The composition of the films is given based on the batch composition; $a_{f\perp}$ was determined from x-ray measurements; it was assumed that $a_s = 12.383$ Å; the values of h_{111} and c_{44} are taken from Table I for YIG; the refractive index n and the thickness d of the film were calculated from measurements of the mode spectrum, whereupon the mismatch Δ^0 was calculated; Δ' was determined from the mode spectrum; Δn was calculated by (89); and the value of p_{44} by (91). The quantities $R_{\max}$ ($\theta = 0$, $\phi = 90°$), l_0, and α were found by displacing the exit prism, and $|k|$ and $|\Delta'|$ were found from (90).

The positive values of p_{44} for two films (Nos. 2 and 6) involve misprints in Ref. 86. Apparently the values of Δ^0 and Δ' have been interchanged for film No. 2, and an incorrect value of $a_{f\perp}$ has been given for film No. 6. These films were not taken into account in calculating p_{44}. Probably the appreciable deviations of the values of p_{44} from the mean for different films arise from lack of allowance for magnetooptic birefringence in these studies. Attention is called to the better agreement between the value of the mismatch found form the mode spectrum and from mode conversion.

Conversion of guided modes has been studied experimentally in Refs. 38, 45, 46, and 84–91. Figure 13 shows the

TABLE III.

No.	Film Composition x	Film Composition y	$a_{f\perp}$ Å	$u_{\parallel}\ 10^{-4}$	n_0	d, μm	$\Delta^0\ 10^{-5}$	$\Delta'\ 10^{-5}$	$\Delta n\ 10^{-5}$	$-p_{44}\ 10^{-1}$	R_m $\theta=0°$ $\phi=\pi/2$	l_0, mm	$\lvert\Delta'\rvert\ 10^{-5}$	α, dB/cm (TE$_0$)	References
	$Y_{3-x}Tb_xFe_{5-y}Al_yO_{12}$														
1	2,07	0,43	12,3868	−1,7	2,192	7,4	3,8	−9,3	13,1	0,4	0,59	4,3	8,6	13	38, 86
2	1,59	0,33	12,3842	−0,5	2,189	5,7	3,7	8,2	−4,5	−0,45	0,95	3,5	3,7	6	Ditto
3	1,23	0,25	12,3849	−0,8	1,196	6,3	6,2	0,0	6,2	0,38	1,0	3,2	0,0	5,6	» »
4	1,11	0,28	12,3769	2,7	2,189	6,8	5,0	29	−24	0,46	0,3	1,6	30,1	7,6	» »
5	1,27	0,25	12,3830	0,0	2,193	5,1	11,4	11,3	0,1	—	0,76	2,5	11,3	5,6	» »
6	1,34	0,26	12,3841	−0,48	2,195	8,2	2,9	5,9	−3	−0,32	0,93	2,6	5,9	5,9	» »
7	1,09	0,29	12,3815	0,66	2,188	5,6	8,6	14	−5,4	0,42	0,74	2,1	14	5,5	» »
8	1,09	0,29	12,3778	2,27	2,19	6,7	5,3	29	−23,7	0,54	0,3	1,7	28,3	—	45
9	1,10	0,28	12,3815	0,66	2,19	6,1	7,3	14	−6,7	0,52	0,75	2,1	13,7	—	Ditto
10	1,22	0,29	12,3841	−0,48	2,19	7,6	3,8	1	2,8	0,35	0,95	2,3	5,6	—	» »
	$Gd_xY_{3-x}Fe_{5-y}Ga_yO_{12}$														
11	0,45	0,9	12,3848	−0,79	2,147	5,3	10,7	3,8	6,9	0,48	0,95	3,4	3,8	—	84, 87
12	0,5	1,0	12,3838	−0,35	2,15	—	19,7	16,7	3,0	0,47	0,34	2,8	16,7	—	Ditto
13	0,4	1,0	12,3830	0,0	2,15	3,4	36	36	0	—	0,15	1,5	35,4	—	» »
14	0,4	1,2	12,3724	4,6	2,13	5,8	5	38	−33	0,4	0,02	1,5	38	6	» »
15	0,45	0,9	12,3850	−0,87	2,15	4,5	16,1	8,1	8	0,5	0,75	5,8	5	—	87
16	—	—	12,3846	−0,7	2,15	—	18,4	12	6,4	0,5	0,47	3,4	12,4	—	Ditto
17	0,62	1,0	12,3841	−0,48	2,145	5,4	10	5,1	4,9	0,56	0,85	4,8	4,7	5,7	88
18	0,7	0,995	12,3884	−2,4	2,147	7,6	3,6	−12,5	16,1	0,37	0,49	3,3	12,5	6,5	Ditto
19	0,677	1,0	12,3862	−1,4	2,146	9,2	2	−8,8	10,8	0,42	0,64	3,9	8,9	6,0	» »
20	0,69	1,014	12,3882	−2,3	2,148	4,2	19,6	2,0	17,6	0,42	0,97	5,0	2,0	5,2	» »
21	0,674	1,05	12,3870	−1,75	2,147	4,4	17,3	2,1	15,2	0,47	0,97	5,0	2,0	5,4	» »
22	0,687	1,03	12,3859	−1,27	2,150	5,5	8,7	−1,7	10,4	0,45	0,98	5,1	1,6	7,0	» »
23	0,7	0,978	12,3871	−1,79	2,145	4,7	14,3	−1,2	15,5	0,47	0,99	4,6	1,3	5,0	» »
24	$Eu_{1.5}Y_{1.5}Al_{0.63}Fe_{4.37}O_{12}$		12,3913	−3,6	2,13	7,3	35,3	3,95	31,4	0,49	—	—	—	—	87

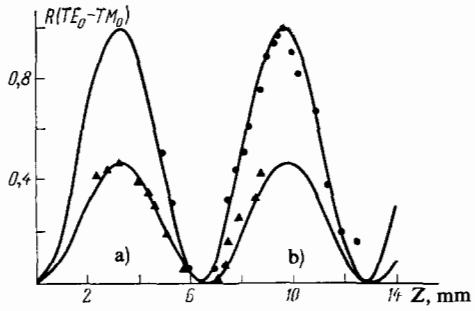

FIG. 13. $TE_0 \rightarrow TM_0$ mode conversion. a) In film No. 3 in Table III (Faraday geometry,[86] curve—calculation by (41) with $\Delta' = 0$ and $|k| = 9\times10^{-5}$); b) in a film close in composition to No. 2 in Table III (angles of the magnetization: $\theta = 45°$ and $\phi = 0°$; curve—calculation by (41) with $|\Delta'| = 1.3\times10^{-5}$ and $|k| = 6\times10^{-5}$.

experimental relationship of the conversion coefficient for a Faraday geometry to the propagation distance for film No. 3 from Table III, from which we can find that $l = 3.2$ mm and $R_{max} = 1$. Upon using (90), we find that $\Delta' = 0$ and $|k| = 9\times10^{-5}$. According to (50) and (56), for the given geometry ($\theta = 0$, $\phi = 90°$), we have

$$\varepsilon_1 - \varepsilon_2 = \frac{\Delta g}{2} M^2 + 2p_{44}\varepsilon_0^2 (u_{\parallel} - u_{\perp}). \quad (92)$$

If we assume that the light propagates along the ⟨110⟩ axis. Since mode synchronization requires that $\varepsilon_1 > \varepsilon_2$, then if we assume that Δg is small enough, we find that the film must be in the compressed state ($u_{\parallel} < 0$). This is confirmed by x-ray measurements (see Table III). We note that a non-zero nondiagonal component of the symmetric part of $\hat{\varepsilon}$ exists in the given geometry, namely $\varepsilon_6 = \sqrt{2}\Delta g/6$. Thus the coupling coefficient is determined not only by the Faraday rotation constant, but also by the anisotropy of the Voigt effect.

Figure 13 shows the variations of $R(z)$ when the magnetization direction was defined by the angles $\theta = 45°$ and $\phi = 0$ (Fig. 7) for a film close in composition to No. 2 in Table III. In the given geometry the conversion arises, as one can find from (56), from the nondiagonal component $\varepsilon_6 = g_{44} + 0.2\Delta g$. We can find from the experimental $R(z)$ relationship that $|\Delta'| = 1.3\times10^{-4}$ and $|k| = 6\times10^{-5}$.

An important characteristic of a waveguide is the magnitude of the losses. The total losses are mainly composed of absorption in the material of the film and of scattering, both at the boundaries and in the bulk of the film. Since these mechanisms have different dependences on the mode order (owing to the differing distribution of the field in a transverse cross-section of the waveguide for modes of different orders), one can distinguish their contributions to the overall losses.[91] Figure 14 shows the relation of the overall losses to the mode order and indicates the contributions from the different mechanisms.

Mode conversion was studied in Ref. 89 with account taken of the absorption α_e and α_h of the TE and TM modes respectively. In this case the conversion coefficient will be determined by the expression

$$R(z) = \exp[-(\alpha_e + \alpha_h) z] \cdot \frac{4|k|^2}{L^2} \times \left\{ \sin^2\left(\frac{Lz}{2}\cos\frac{\psi}{2}\right) + \sin h^2\left(\frac{Lz}{2}\sin\frac{\psi}{2}\right)\right\}. \quad (93)$$

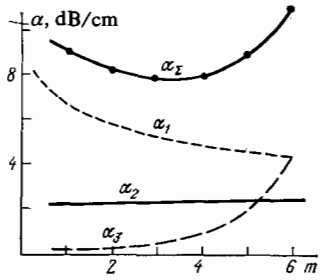

FIG. 14. Losses for modes of different orders. α_Σ—total losses, α_1—absorption in the film, α_2—scattering in the film, α_3—scattering at the boundaries.

Here we have

$$L = \{[4\nu^2 - \Delta\alpha^2]^2 + 4(\Delta' \cdot \Delta\alpha)^2\}^{1/4},$$

$$\psi = -\tan^{-1}\left[\frac{2\Delta' \cdot \Delta\alpha}{4\nu^2 - \Delta\alpha^2}\right], \quad \Delta\alpha = \alpha_e - \alpha_h.$$

If $\Delta\alpha = 0$, then (93) reduces to (41), apart from the exponential factor $\exp(-2\alpha z)$ (omitted in error in Ref. 89). Figure 15 shows the experimental dependence of the conversion (film No. 14, Table III) on the propagation distance and the theoretical dependence according to (93) for $\alpha_e = 6$ dB/cm, $\alpha_h = 11$ dB/cm, $kk_0 = 75$ deg/cm, $\Delta' k_0 = 1200$ deg/cm. The increase in the conversion maximum is explained by the difference in losses of the TE and TM modes.

References 84 and 88–90 have studied the dependence of the conversion on an external magnetic field. The relationships are described by (41) and (56). Figure 16 shows the dependence of the conversion on the magnitude of a magnetic field applied along the x axis (perpendicular to the film). The conversion passes through a maximum (when the magnetization lies at angles $\theta = 45°$ and $\phi = 0°$) and it vanishes at fields above ~800 Oe (when $\theta = 90°$), as is implied by (56). Figure 16 shows the theoretical dependences obtained under the assumption that $\Delta g = 0$ and $\sin\theta = H_x/H_u$, where H_u is the uniaxial anisotropy field (~820 Oe for the given film). The agreement with experiment is good.

Nonreciprocal mode conversion in epitaxial films of ferrite garnet has been found[90] upon reversing the direction of a magnetic field along the direction of propagation (Fig. 17). It was explained by a combination of reciprocal conversion in the substrate owing to optical anisotropy caused by stresses and nonreciprocal conversion in the film caused by the Faraday effect. Figure 18 shows the dependence of the

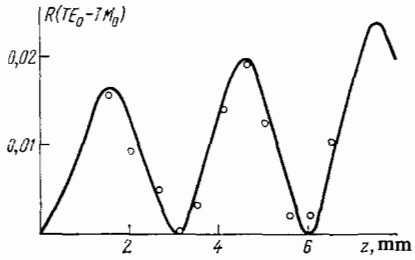

FIG. 15. $TE_0 \rightarrow TM_0$ mode conversion for film No. 14 in Table III.[84,89] Curve—calculation for $\alpha_e = 6$ dB/cm, $\alpha_h = 11$ dB/cm, $K = 2.4\times10^{-5}$, $|\Delta'| = 3.8\times10^{-4}$ by Eq. (93).

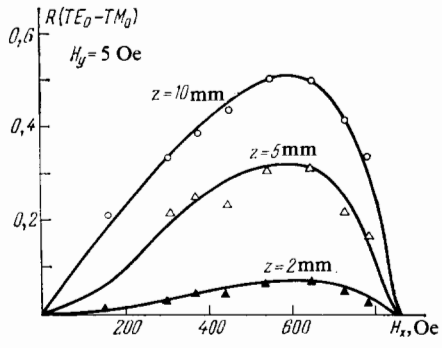

FIG. 16. Conversion as a function of the magnitude of the constant magnetic field perpendicular to film No. 11 in Table III.[84,89] Curves—calculation by (41) and (56) for $K = 1.4\times10^{-3}$, $\Delta' = 4.7\times10^{-5}$, $\Delta g = 0$, sin $\phi = H_x/H_u$, $H_u = 820$ Oe.

conversion of the magnitude and direction of the field for several pairs of modes of the same order. The decrease in R/R_{max} with increasing mode order confirms the hypothesis that the nature of the nonreciprocity in this case involves birefringence in the substrate.

In Ref. 46 a considerable nonreciprocity ($R^+ = 0.93$; $R^- = 0.09$) was observed in an inhomogeneous magnetic field. The authors explained its origin by the existence of magnetic birefringence in some parts of the film and gyrotropy in others.

Let us note some further experimental studies on waveguide propagation of light in ferrite films. An influence of coupling between modes on the mode spectrum was demonstrated in Ref. 92. As we have already noted above (see Sec. 2), coupling leads to a change in the propagation constants according to (44) and to "hybridization" of modes. Both these effects were discovered with a birefringent rutile prism, which split each hybrid mode into two rays corresponding to its components having different polarizations.

In Ref. 7 the absorption spectrum was studied of epitaxial films of ferrite garnets by the method of waveguide optics. Waveguide optics was first applied for continuous recording of an absorption spectrum. This made it possible to reveal the features of the spectrum that cannot be detected by ordinary methods of absorption spectroscopy (owing to the small thickness and absorption of the film). Figure 19 shows the transmission spectrum obtained by transilluminating the film and by the waveguide method.[7]

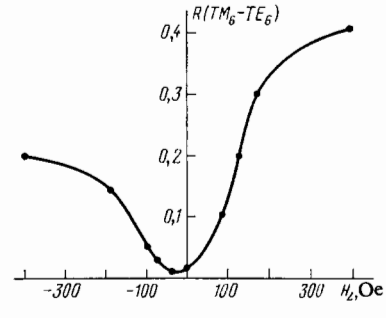

FIG. 17. $TM_6 \rightarrow TE_6$ mode conversion as a function of the magnitude of the longitudinal magnetic field for a film of $Y_3Sc_{0.37}Fe_{3.61}Ga_{1.02}O_{12}$ ~9-μm thick.[90]

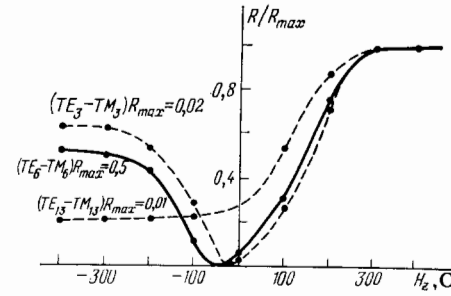

FIG. 18. Nonreciprocal mode conversion for a film of $Y_3Sc_{0.37}Fe_{3.61}Ga_{1.02}O_{12}$.

A promising line for designing more highly miniaturized elements of integrated optics is to use multilayer waveguides. The first step in this direction is the synthesis and study of bilayer epitaxial films.[56–58,93,94]

It was proposed[56] to employ a double epitaxial heterostructure to obtain quasisynchronization of modes. A film is grown on a substrate of gadolinium gallium garnet that consists of two layers. The layer closest to the substrate has a refractive index somewhat smaller than in the next layer. the propagation constants without allowance for anisotropy and gyrotropy can be calculated by using the dispersion equations for a four-layer waveguide structure derived in Ref. 58. In the region of β values not too close to the refractive index of the intermediate layer, such a waveguide structure behaves like an ordinary three-layer waveguide in which the intermediate layer plays the role of the substrate. Since the range of β values in such a structure is restricted to the narrow region between the two refractive indices of the film, then evidently, the difference between the wave numbers of the TE and TM modes of the same order (Δ^0) will be smaller than without the intermediate layer. This has been verified experimentally with the heterostructure GdGa–YbScGaFe–YbScFe,[56] in which $R = 0.5$ was obtained for the first-order modes.

The value $R = 0.96$ was attained in Ref. 57 for a similar structure (the upper layer of the film also contained gallium, but in smaller concentration than in the intermediate layer).

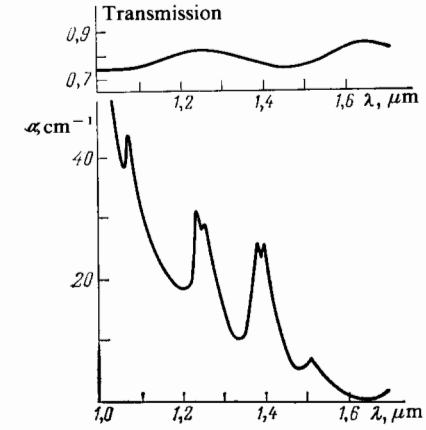

FIG. 19. Dispersion relationships of the transmission in ordinary transillumination and the absorption coefficients in waveguide propagation for $(YSmLuCa)_3(FeGa)_5O_{12}$.[7]

Such a large conversion (instead of the calculated $R = 0.2$ in the case of an isotropic structure) arises from the additional coming together of the modes owing to the photoelastic anisotropy in the upper layer.

It was noted in Ref. 57 that, with a refractive-index difference of the two layers of the film equal to 0.005, one can obtain a conversion coefficient $R = 0.95$ without anisotropy with a specific Faraday rotation of 200 deg/cm. However, too rigid requirements are placed here on the control of the refractive index of the two layers of the heterostructure. The requirements on the control of the refractive indices can be lowered by depositing a coating with a sufficiently high refractive index (equal in the limit to the refractive index of the intermediate layer).

As will be eivdent from Sec. 4, in devices using coupling of waveguide modes, it is essential to have as great as possible a conversion between them. In closing this section, let us list the possible ways of increasing mode conversion.[56] It can be increased by using: 1) an anisotropic material in the waveguide structure; 2) the Voigt effect; 3) a metallic top layer separated from the waveguide by an intermediate film[95]; 4) a periodic structure; 5) materials with a strong Faraday rotation; and 6) two-layer films.

4. FERRITE FILMS IN FUNCTIONAL ELEMENTS OF INTEGRATED OPTICS

Although the first demonstration of the possible application of epitaxial films of ferrite garnets in integrated optics was a modulator (switch),[51] they are most promising for building nonreciprocal elements, which will mainly be treated here.

The principles of constructing nonreciprocal elements of integrted optics have been developed in Refs. 31b, 33, 39, 43, 48, 50, 54, 55, 57, and 96–103. Usually the main elements of such devices as an isolator, a circulator, etc., is the so-called unidirectional mode converter (UMC), which in the ideal case has $R^+ = 0$ and $R^- = 1$. As was shown in Sec. 2, nonreciprocal conversion can be associated with nonreciprocity of the mismatch or of the coupling coefficient. In all UMCs proposed up to now, nonreciprocity of the coupling coefficient has been employed. As is clear from Sec. 2, one can obtain a nonreciprocal coupling coefficient by combining a certain optical anisotropy with the appropriate gyrotropy. Such a combination can be of the cascade[55] or single-section[98] type. If we base our discussion on the variants proposed up to the present, the single-section combinations have the advantage with respect to miniaturization, but they are as yet less practical commercially.

Now let us proceed to discuss the concrete variants of UMCs. Figure 20 shows an isolator proposed in Ref. 48. It was proposed to obtain a nonreciprocal coupling coefficient by gyrotropy of a ferrite film and anisotropy of the top layer made of a monocrystal of lithium iodate. However, experimentally it was not possible to obtain nonreciprocal conversion in this system. As was shown in Refs. 33 and 48, the coupling coefficient in such a system depends very sharply on the size of the air gap between the film and the top layer.

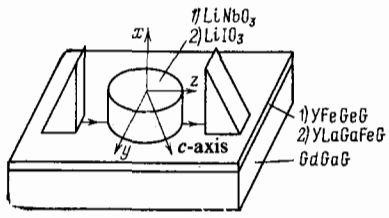

FIG. 20. Isolator of the "semileaky type"[50] (variant 1) and a UMC[48] (2).

The unfavorable choice of the material for the top layer, which is hygroscopic, apparently led to the negative result.

A single-section system was experimentally demonstrated for the first time in Ref. 99 with a nonreciprocity of conversion of 7 dB (Fig. 21). A film of BiTmFeGa garnet was pressed onto a diffusion waveguide based on lithium niobate until optical contact was made. In the region of the latter, either a two-layer waveguide arose, or a system of two coupled waveguides, depending on the size of the air gap between the diffusion waveguide and the magnetic film. In both cases, the energy partially propagated along the magnetic film, where conversion arose from the Faraday effect. It was possible by varying such parameters as the pressure on the film and the length of optical contact to obtain a nonreciprocityofconversionin$(1 - R^+)(1 - R^-) \equiv I^+/I^-$($I^+$and I^- are the intensities of themodes when propagating in the forward (+) and backward (−) directions) of 7 dB for the zero-order modes at $\lambda = 1.15$ μm and a length of optical contact ~ 3 mm.

Increase in the nonreciprocity requires a more careful choice of the parameters of the diffusion waveguide and the magnetic film. On the whole, this nonreciprocal system has the advantage over those discussed in Ref. 48 that one can construct immediately beyond it an electro- or acoustooptical modulator using the same diffusion waveguide.

An UMC of the cascade type has been described in Ref. 101. It consists of two sections of the same epitaxial garnet film. A Faraday geometry is realized in one section by using an external magnetic field, while in the other section another source of an external magnetic field creates the geometry of the Voigt effect. The match of phase velocities of the modes necessary for operation of the UMC was obtained by deformation of the film during epitaxial growth by selecting the appropriate mismatch of the lattice parameters of the film and the substrate (see Sec. 3). by using (36), (37), (45), (56), and (59), one can find that the following expressions for the quantities entering into (68) hold for modes far from cutoff:

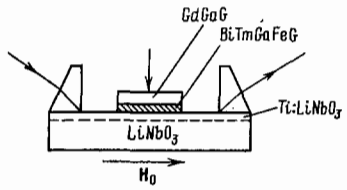

FIG. 21. Isolator with nonreciprocity of conversion of 7 dB.[99]

$$k = fM\cos\theta\sin\phi + ig_{44}M^2\sin 2\theta\cos\phi,$$
$$\Delta' = 2g_{44}M^2(\sin^2\theta - \cos^2\theta\cos^2\phi), \quad (94)$$
$$\nu^2 = (fM)^2\cos^2\theta\sin^2\phi + g_{44}^2M^4(1-\cos^2\theta\sin^2\phi)^2.$$

Here we have assumed that $\Delta^0 = \Delta g = 0$. Upon substituting into (68) the values of k and ν from (94) for the two sections of the UMC in which the directions of the magnetization are defined by the angles $\theta_1 = 0$, $\phi_1 = \pi/2$, and $\theta_2 = \pi/8$, $\phi_2 = 0$, while the length of the sections is $z_1 = \pi/4\nu_1$ and $z_2 = \pi/2\nu_2$, we find that the overall matrix of the two-section UMC will have the following forms for the forward (+) and backward (−) waves:

$$T^+ = T_1^+T_2 = i\begin{bmatrix} -1 & 0 \\ 0 & 1 \end{bmatrix}, \quad T^- = T_1^-T_2 = i\begin{bmatrix} 0 & 1 \\ 1 & 0 \end{bmatrix}.$$

Thus full conversion occurs for the backward wave and no conversion for the forward wave.

A UMC has been realized that is based on a film made of YGdGaFe garnet 5-μm thick grown on a substrate of gadolinium gallium garnet with {111} orientation. The light propagated along the ⟨110⟩ direction. The Faraday section of the UMC was 3.5-mm long, and the section with the Voigt geometry 12 mm long. The study demonstrated nonreciprocity of conversion, but gave no quantitative estimate of it.

An isolator can be built based on a UMC by placing mode filters at both ends of it.[55] As was shown in Ref. 104, the filter transmitting only the TE modes can be a metallic coating. The damping of the TM modes for an aluminum coating is $\gtrsim 60$ dB/mm, whereas the losses for the TE modes are < 1 dB/mm. One can diminish the absorption of the TE modes by depositing a dielectric film between the waveguide and the metal.

Another type of isolator ws proposed in Ref. 43 and realized in Ref. 50 (Fig. 20). It is based on using waveguides of the semileaky type (see Secs. 2 and 3). the nonreciprocity obtained in a waveguide structure made of a film of yttrium iron garnet with a top layer of a crystal of lithium niobate amounted to 10 dB at a distance of 1 cm for $\lambda = 1.15$ μm. The main feature of this isolator is that a guided mode interacts with a radiative mode in it, rather than with a guided mode. In this case the strict requirements on mode syncrhonization, length of the isolator, thickness of the film, and quality of optical contct that exist for devices that employ conversion between guided modes are considerably relaxed. For example, a semileaky-type isolator cn operate with any propagation length. That is, doubling the length leads to doubling the nonreciprocity. We note that it is imposssible to obtain complete nonreciprocity in such an isolator, since the conversion varies exponentially (see (71)). In Ref. 50 a nonreciprocity of 10 dB was obtained in a length of 1 cm, which is comparable with the results obtained in conversion of guided modes (10.1 dB in a lnegth of 8 mm[46]). The requirements on the optical contact are also less strict in thcase of a semileaky-type isolator.

Despite all the merits presented above of a semileaky-type isolator, it is by no means universal, mainly because of the complexity of construction, cost, the need for having two high-quality single crystals, lack of commrcial feasibility (poor fit with planar technology), etc. It is also unclear to what extentone can increase the nonreciprocity without substantial complication of the technology. We should note also the large losses introduced for the forward wave of ~ 10.1 dB for a nonreciprocity of 9.9 dB.

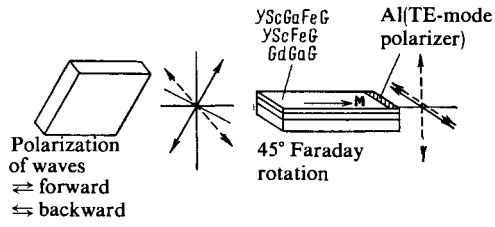

FIG. 22. Isolator employing a bilayer film.[57]

Apparently many of the defects pointed out above can be eliminated in an isolator based on a two-layer film. One of the variants of such an isolator was proposed in Ref. 57. Figure 22 shows the fundamental scheme of it. The light from a semiconductor laser passes through the two-layer-film, whose plane lies at a 45° angle to the plane of polarization of the laser. After rotation by 45° in the film, the polarization of the light corresponds to the polarization of the TE modes and the radiation passes through a filter in the form of a metallic coating. The backward wave in the form of TE polarization (the filter does not transmit TM polarization) passes through the two-layer film with a rotation of the plane of polarization by 45° and is incident on the semiconductor laser. Since the angle between the plane of polarization of the laser and the backward wave amounts to 90°, th backward radiation does not affect the characteristics of the radiation of the laser. The operation of the two-layer film is based on almost complete TE ⇌ Tm conversion (see Sec. 3).

An isolator was proposed[97] for TM modes that used nonreciprocity of the phase shift δ_e as determined by (36), and which did not require mode conversion. The isolator has the structure of an interferometer (Fig. 23) in which the phase nonreciporcity is converted into amplitude nonreciprocity. This isolator has not beenrealized in practice.

A theoretical detailed analysis has been performed[100] of a five-layer waveguide structure consisting of two isotropic dielectric waveguides coupled by a gyrotropic and/or anisotropic medium. It was shown that one can design an optical circulator based on this structure that does not require a mode separator at the input and output, and an isolator that does not require mode filters.

It has been proposed[103] to use magnetic materials with a large natural optical anisotropy, such as $YFeO_3$ and $FeBO_3$, for designing UMCs. The practical realization of different variants of the devices from REfs. 100 and 103 will depend on the future development of thin-film technology, both

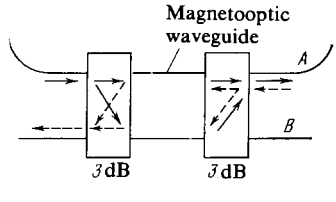

FIG. 23. Isolator based on the principle of nonreciprocal phase shift.[97]

with respect to attaining high quality of waveguide structures and to possible strit control of their parameters.

In closing this section, we shall take up some possible applications of epitaxial ferrite garnet films that do not pertain to nonreciprocal elements. A deflector was described in Ref. 105 that employs a periodic grating made of stripe domains (Sec. 3). The light propagating in waveguide fashion in the film was diffracted by the grating of stripe domains, which had a sign-variant component of the magnetization in the plane of the film. A rutile prism was used to excite the TE mode, which was diffracted by the polarization grating of stripe domains. The light was converted to the TM_1 mode and deflected by diffraction at a maximum angle of 3° with a maximum efficiency of 15% (the ratio of intensities of the deflected light to the total transmitted light). A filmwas used of thickness 4.4 μm of composition $Gd_{0.45}Y_{2.55}Fe_{4.2}Ga_{0.8}O_{12}$. The variation of the intensity of the diffracted light as a function of the angle of incidence can be calculated by Eq. (41), where in this case one should assume for a rectangular profile of variation of the magnetization: $R = I/I_0$, $|k| = |F_0|/2\pi$, $z = L$, $\Delta' = 2\pi(\Phi - \Phi_B)/D$. Here I_0 and I are respectively the intensities of the incident and diffracted light, F_0 is the specific Faraday rotation, L, is the interaction length, D is the period of the stripe domains, Φ is the angle of incidence in the plane of the film with respect to the domain walls, and Φ_B is the Bragg angle, as determined by the relationship $\sin \Phi_B = \lambda (2nD)^{-1}$.

Figure 24 shows the I/I_B relationship, where I_B is the intensity forthe Bragg angle. The calculated curve corresponds to the parameters $L = 4$ mm, $F_0 = 130$ deg/cm, and $D = 25\,\mu$m. Here the theoretical value of the diffraction efficiency is 30%. The curves in Fig. 24 correspond to an efficiency of 3%. By increasing the distance to 1 cm, a maximum efficiency of 15% could be obtained. To increase the efficiency, one should use films with better regularity of domain structure and with higher values of the Q-factor $M_1 = F_0/\alpha$.

In Ref. 106 a grating made of stripe domains in an epitaxial film of BiYbFe garnet was used to introduce light into a glass waveguide. The efficiency of diffraction in the first order for a film 0.41-μm thick was 0.41%. The intensity of the light introduced into the waveguide was diminished by 72% by using an external pulsed magnetic field, which altered the period of the domain structure.

It has been proposed[107] to employ epitaxial films of garnets to design integrated-optics logicl elements. By the estimates of the author, these have dimensions ($\sim 23\,\mu$m) far smaller than the analogous elements based on electrooptical materials (millimeters).

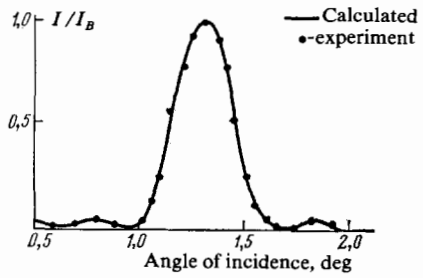

FIG. 24. Diffraction of "waveguide" light by stripe domains.[105]

As we have already mentioned at the beginning of this section, epitaxial films of ferrite garnets can find application in amplitude modulators,[44,51,53] whose quality factor is comparable with the best electrooptic modulators (~ 1 mW/MHz), while the limiting frequency values can lie abovė 1 GHz. We shall not take up the discussion of modulators here, since their operation has been described and their characteristics compared with acousto- and electrooptical modulators in the review of Ref. 1. We shall call attention only to Ref. 108, in which studies were begun on the interaction of "waveguide" light with surface spin waves. In an epitaxial film of yttrium iron garnet with collinear propagation of the light and the spin wave, a 4% conversion was obtained at a frequency ~ 4 GHz. Attaining a greater conversion with decreased interaction length hinges on the possibility of growing films with a narrow width of ferromagnetic resonance and a larger Faraday rotation.

One of the main problems on the pathway to using epitaxial films of ferrite garnets in integrated optics remains the large optical losses. As we see from Table III, the best result, 5 dB/cm, greatly exceeds the losses in massive specimens of yttrium garnet, .26 dB/cm.[109-110] Apparently this involves the preesence of lead in the film. If the device is based on using solely the Faraday effect, then the losses introduced are governed by the ratio of the Faraday rotation to thelosses (M_2). Introduction into the garnets of ions of Bi^{3+} and/or Pr^{3+}, while appreciably increasing the Faraday rotation, unfortunately also increases the losses (see Table II). Improvement of the situation is made possible by increasing the wavelength of the radiation and cooling.[109] We note that an increase in the wavelength, e.g., to 1.55 μm, simultaneously leads to increase in M_2 and to a considerable decrease in the losses in the optical fiber.

CONCLUSION

We have discussed the effects that can be observed (or have already been observed) in waveguide structures containing gyrotropic media. We wish to stress again that waveguide magnetooptics can solve fundamental, materials-science, and applied problems. The fundamental problems that waveguide magnetooptics can clarify include, e.g., the problem of the contribution of the magnetic susceptibility to magnetooptic effects.

From the standpoint of characterizing thin-film materials, waveguide magnetooptics is a very accurate method of determining such parameters as the thickness, the refractive index, the birefringence, the Faraday rotation, the constants of the photoelastic tensor and the magnetooptic tensor of second order in the magnetization, etc., some of which are difficult, and sometime even impossible to obtain by other methods.

The potentialities of applying the effects of waveguide magnetooptics are extremely varied. The Faraday and Voigt effects can be employed to modulate light with small magnetic fields (~ 0.1 Oe). On the level of nonreciprocity, one

can design isolators, circulators, and gyrators in an integrated-optics form. Isolators based on epitaxial garnet films already can find appliction in optical communications systems to diminish the strong noise arising from reflected radiation.

At this stage it is difficult to draw concrete conclusions on the future application of magnetic materials in integrated optics. The most likely sphere of their application, as we view it, is in nonreciprocal uncoupling elements. We do not agree wth the opinion put forth in Ref. 3 that nonreciprocal devices are not necessary in integrated-optics circuits. Although reflections from joints in thin-film devices can be substantially diminished with joints of the "slanted edge" type and not all the reflected energy forms a backward wave in the waveguide, one cannot state that other inhomogeneities in the optical circuit (e.g., modulators, couplings with fibers, etc.) will not lead to forming a backward wave of considerable power. Moreover, it has already been shown experimentally[9] that, in coupling a semiconductor laser with a fiber, a nonreciprocal device is necessary to eliminate the amplitude and frequency oscillations caused by the reflected wave.

The authors thank V. N. Gridnev, E. L. Ivcheko, O.G. Rutkin, R. v. Pisarev, and A. S. Trifonov for useful discussions of this article.

[1]T. Tamir, ed., Integrated Optices, 2nd edn., Springer-Verlag, Berlin, 1979 (Russ. Transl. of 1st eds., Mir, M., 1978).
[2]A. M. Goncharenko, L. N. Deryugin, A. M. Prokhorov, A. M. Prokhorov, and g. P. Shipulo, Zh. Prikl. Spektrosk. **24**, 987 (1978).
[3]P. K. Tien, Rev. Mod. Phys. **49**, 361 (1977).
[4]H. F. Taylor and A. Yariv, Proc. IEEE **62**, 1044 (1974) (Russ. Transl., TIIÉR **62**, No. 8, 4 (1974)]..
[5]W. D. Westwood, Can. J. Phys. **57**, 1247 (1979).
[6]K. Tanaka, Appl. Phys. Lett. **34**, 672 (1979).
[7]M. Olivier, J. C. Penzin, and J. S. Danel, Appl. Phys. Lett. **38**, 79 (1981).
[8]K. Mitsunaga, M. Musuda, and J. Koyama, Opt. Commun. **27**, 361 (1978); K. P. Birch, *ibid.* **43**, 79 (1982).
[9]I. Ikushima and M. Maedo, IEEE J. Quantum Electron. **QE-14**, 331 (1978); O. Hirota and Y. Suematsu, *ibid.* **QE-15**, 142 (1979); T. Matsumoto, Electron. Lett. **15**, 625 (1979); G. Wenke and G. Elze, J. Opt. Commun. **2**, 128 (1981).
[10]V. P. Silin and A. A. Rukhadze, Élektromagnitnye svoĭsta plazmy i plazmopodobnykh sred (Electromagnetic Properties of Plasmas and Plasma-Like Media), Gosatomizdat, M., 1961; A. M. Ignatov and A. A. Rukhadze, Usp. Fiz. Nauk **135**, 171 (1981) [Sov. Phys. Usp. **24**, 795 (1981]; S. I. Pekar, Kristallooptika i dobavochnye svetovye volny. (Naukova Dumka, Kiev, 1982). [Engl. Transl. Crystal Optics and Additional Light Waves, Benjamin, Reading, Mass., 1983].
[11]S. R. de Groot and L. G. Suttorp, Foundations of Electrodynamics, North-Holland, Amsterdam, 1972 (Russ. Transl., Nauka, M., 1982); S. Kelikh, Molekulyarnaya nelineĭnaya optika (Molecular Nonlinear Optics), Nauka, M., 1981; D. J. Caldwell and H. Eyring, The Theory of Optical Activity, Wiley, Interscience, 1971
[12]V. M. Agranovich and V. L. Ginzburg, Kristallooptika s uchetom prostranstvennoĭ dispersii i teoriya éksitonov (Crystal Optics with Account Taken of Spatial Disperison and the Theory of Excitons), Nauka, M., 1979 (Engl. Transl. of 1969 edn., Spatial Dispersion in Crystal Optics and the Theory of Excitons, Interscience, London, 1966).
[13]V. L. Levich, Yu.A. Vdovin, and V. A. Myamlin, Kurs teoreticheskoĭ fiziki (Course in Theoretical Physics), Fizmatgiz, M., 1962.
[14]F.I. Fedorov, Teoriya girotropii (Theory of Gyrotropy), Nauka i tekhnika, Minsk, 1976.
[15]L. D. Landau and E. M. Lifshitz, Élektrodinamika sploshnykh sred (Electrodynamics of Continuous Media), Nauka, M., 1982 (Engl. Transl. of earlier edn., Pergamon, Oxford, 1960).
[16]R. M. Hornreich and S. Shtrikman, Phys. Rev. **171**, 1065 (1968).
[17]P. S. Pershan, J. Appl. Phys. **38**, 1482 (1967).
[18]G. S. Krinchik, Fizika magnitnykh yavlenii (Physics of Magnetic Phenomena), Izd-vo Mosk. un-ta M., 1976; G. S. Krinchik, S. v. Koptsik, and E. A. Gan'shina, Fiz. Tverd. Tela (Leningrad) **24**, 1270 (1982) [Sov. Phys. Solid State **24**, 721 (1982)].
[19]A. N. Ageev, V. N. Gridnev, O. G. Rutkin, and G. A. Smolenskiĭ, Fiz. Tverd. Tela (Leningrad) **25**, 478 (1983) [Sov. Phys. Solid State **25**, 270 (1983)].
[20]J. F. Nye, Physical Properties of Crystals, Clarendon Press, Oxford, 1957 (Russ. Transl., IL, M., 1960).
[21]G. A. Smolenskiĭ, R. V. Pisarev, and I. G. Siniĭ, Usp. Fiz. Nauk **116**, 231 (1975) [Sov. Phys. Usp. **18**, 410 (1975)].
[22]J. F. Dillon *et al.*, J. Appl. Phys. **41**, 4613 (1970).
[23]L. D. Dedukh and V. I. Nikitenko, Fiz. Tverd. Tela (Leningrad) **12**, 1768 (1970) [Sov. Phys. Solid State **12**, 1400 (1970)]; R. T. Lynch and J. F. Dillon, J. Appl. Phys. **44**, 225 (1973); R. V. Pisarev and N. N. Kolpakova, Fiz. Tverd. Tela (Leningrad) **17**, 56 (1975) [Sov. Phys. Solid State **17**, 31 (1975)].
[24]S. H. Wemple, S. L. Blank, and J. A. Semon, Phys. Rev. B **9**, 2134 (1974).
[25]a) G. B. Scott, in: Physics of Magntic Garnets, ed. A. Paoletti, North-Holland, Amsterdam, 1978; b) U. V. Valiev, A. K. Zvezdin, and G. S. Krinchik, Zh. Eksp. Teor. Fiz. **79**, 2356 (1980) [Sov. Phys. JETP **52**, 1193 (1980)].
[26]b) P. Hansen, H. Heitman, and K. Witter, Phys. Rev. B **23**, 6085 (1981); G. S. Krinchik, A. A. Kostyurin, and V. D. Gorbunova, Zh. Eksp. Teor. Fiz. **81** 1037 (1981) [Sov. Phys. JETP **54**, 550 (1981); G. A. Smolenskiĭ, ed., Fizika magnitnykh diélektrikov (Physics of Magnetic Dielectrics), Nauka, L., 1974.
[27]Yu. S. Sirotin and M. P. Shaskol'skaya, Osnovy kristallofiziki (Foundations of Crystal Physics), Nauka, M., 1975, p. 663.
[28]M. Torfeh and H. Le Gall, Phys. Status Solidi A **63**, 247 (1981).
[29]M. W. Muller and M. J. Sun, in: Proc. Symposium on Optical and Acoustic Micro-Electronics, USA, 1974, Brooklyn, N. Y., 1975, p. 393.
[30]G. A. Smolensky, A. N. Ageev, and S. A. Mironov, see Ref. 26a, p. 753.
[31]a) P. K. Tien, Appl. Opt. **20**, 2395 (1971); S. Wang, M. Shah, and J. D. Crow, J. Appl.Phys. **43**, 1861 (1972); S. Wang, M. L. Shah, and J. D. Crow, IEEE J. Quantum Electron. *QE*–8, 212 (1972); b) H. Kogelnik, T. P. Sosnowski, and H. P. Weber, IEEE J. Quantum Electron. **QE-9**, 795 (1973).
[32]S. Yamamoto and Y. Koyamada, J. Appl. Phys. **43**, 5090 (1972); S. Wang and J. D. Crow, *ibid.* **44**, 3232 (1973).
[33]M. J. Sun, M. W. Muller, and W. S. C. Chang, Appl. Opt. **16**, 2986 (1977).
[34]A. Yariv, IEEE J. Quantum Electron. **QE-9**, 919 (1973).
[35]D. Marcuse, Bell syst. Tech. J. **54**, 985 (1975).
[36]D. F. Gia Russo and J. H. Harris, J. Opt. Soc. Am. **63**, 138 (1973).
[37]A. A. Kostyurin, Pis'ma Zh. Tekh. Fiz. **4**, 1477 (1978) [Sov. Tech. Phys. Lett. **4**, 598 (1978)].
[38]M. Torfeh, Thesis, Orsay, 1979.
[39]K. Taki, Y. Miyazaki,a nd Y. Akao, Jpn. J. Appl. Phys. **19**, 925 (1980).
[40]Y. Satomura and M. Matsuhara, IEEE Trans. Microwave Theory Tech., **MTT-22**, 86 (1974).
[41]P. S. Pershan, Phys. Rev. **130**, 919 (1963).
[42]T. P. Sosnowski, Opt. Commun. **4**, 408 (1972); T. P. Sosnowski and H. P. Weber, *ibid.* **7**, 47 (1973)
[43]S. Yamomoto and T. Makimoto, IEEE J. Quantum Electron **QE–12**, 764 (1976).
[44]S. Yamomoto and T. Makimoto, J. Appl. Phys. **48**, 1680 (1977).
[45]L. Courtois, J. M. Desvignes, M. Torfeh, H. Le Gall, and J. P. Castera, in: Rare Earth Conference, Olgebay Park, USA, Sep. 1977.
[46]M. Torfeh, J. M. Desvignes, L. Courtois,and H. Le Gall, J. Appl. Phys. **43**, 1806 (1978).
[47]J. Warner, IEEE Trans. Miwcrowave Theory Tech. **MTT-23**, 70 (1975).
[49]Y. Mayazaki, K. Taki, and Y. Akao, Jpn. J. Appl. Phys. **20**, 935 (1981).
[50]S. T. Kirch, W. A. Biolsi, S. L. Blank, P. K. Tien, R. J. Martin, P. M. Bridenbaugh, and P. Grobbe, J. Appl. Phys. **52**, 3190 (1981).
[51]P. K. Tien, D. P. Schinke, and S. L. Blank, J. Appl. Phys. **45**, 3059 (1974); Appl. Phys. Lett. **21**, 394 (1972).
[52]P. K. tien, Physica (Utrecht) Ser. B and C **89**, 241 (1977).
[53]S. C.-C. Tseng and R. R. Reisinger, Appl. Phys. Lett. **24**, 265 (1975).
[54]R. D. Henry, *ibid.* **26**, 408 (1975).
[55]S. Yamomoto and T. Makimoto, J. Appl. Phys. **45**, 882 (1974).
[56]M. Monerie and A. Leclert, Opt. Commun. **19**, 143 (1976).
[57]A. Shibukawa and M. Kobayashi, Appl. Opt. **20**, 2444 (1981).
[58]M. J. Sun and M. W. Muller, *ibid.* **16**, 814 (1977).
[59]P. K. Tien, R. J. Martin, and S. L. Blank, Appl. Phys. Lett. **21**, 207 (1972).

[60]L. S. Palatnik and I. I. Shapriov, Épitaksial'nye plenki (Epitaxial Films), Nauka, M., 1971; J. W. Matthews, ed., Epitaxial Growth, Academic Press, New York, 1975.
[61]B. J. Besser and J. E. Mee, Mater, Res. Bull. **6**, 1111 (1971).
[62]J. R. Carruthers, J. Cryst. Growth **16**, 45 (1972).
[64]D. C. Miller and R. Caruso, *ibid.* **27**, 274 (1974).
[65]H. Makino *et al.*, AIP Proc. 19th Ann. Conf. (Boston, 1973), No. 18, pt. 1, p. 80 (1974)
[66]C. J. M. Rooijmans, Crystals for Magntic Applications, Springr-Verlag, New York, 1978).
[67]J. W. Matthews and S. Mader, J. Appl. Phys. **41**, 3800 (1970).
[68]S. L. Blank and J. W. Nielsen, J. Cryst. Growth **17**, 302 (1972).
[69]V. F. Dorfman and S. A. Petrushina, Thin Solid Films **62**, 157 (1979).
[70]O. G. Rutkin, A. N. Ageev, and E. L. Dukhovskaya, Zh. Tekh. Fiz. **52**, 2411 (1982) [Sov. Phys. Tech. Phys. **27**, 1486 (1982)].
[71]S. Geller and G. P. Espinosa, J. Appl. Crystallogr. **2**, 86 (1969).
[72]J. W. Matthews and E. Klokholm, AIP Conf. Proc. 18th Annual Conf. (Denver, 1982); Vol. 10, p. 271 (1973).
[73]E. G. Spenser, J. Appl. Phys. **34**, 3059 (1963); **37**, 2194 (1966).
[74]G. F. Dionne, Mater. Res. Bull. **6**, 805 (1971); R. D. Pierce, AIP Conf. Proc. MMM (Chicago, 1971); Vol. 5, p. 91 (1972).
[75]A. M. Balbashov and A. Ya. Chervonenkis, Magnitnye matrialy dlya mikroélektroniki (Magnetic Materials for Microelectronics), Énergiya, M., 1979.
[76]J. Daval and B. Ferrand, Mater. Res. Bull. **10**, 95 (1975); IEEE Trans. Magn. **MAG-11**, 1115 (1975).
[77]S. H. Wemple and J. F. Dillon, Appl. Phys. Lett. **22**, 331 (1973); S. Visnovsky and R. Krishnan, Physica (Utrecht) Ser. B and C **89**, 73 (1977).
[78]H. P. Weber, Appl. Opt. **12**, 755 (1973).
[79]M. J. Sun, Appl. Phys. Lett. **33**, 291 (1978); A. N. Ageev, E. V. Mokrushina, and A. S. Trifonov, Zh. Tekh. Fiz. **52**, 2044 (1982) [Sov. Phys. Tech. Phys. **27**, 1255 (1982)].
[80]R. D. Henry and E. C. Whitcomb, Mater. Res. Bull. **10**, 681 (1975).
[81]A. N. Ageev, E. v. Mokrushina, and A. P. Kirmenskiĭ, Fiz. Tverd. Tela (Leningrad) **24**, 1501 (1982) [Sov. Phys. Solid State **24**, 858 (1982)].
[82]J. M. Robertson, J. Cryst. Growth **7**, 233 (1978).
[83]M. Monerie and A. Leclert, Opt. Commun. **16**, 408 (1976).
[84]G. Hepner and J. P. Castera, AIP Conf. Proc. 21st Ann. Conf. MMM (Philadelphia, 1975); Vol. 29, p. 658 (1975).
[85]P. G. Van Engen, J. Appl. Phys. **49**, 4660 (1978).
[86]M. Torfeh, J. M. Desvignes, and H. Le Gall, in: Intern. Colloquium on Magnetic Films and Surfaces, University of Lodz, 1979, p. 127.
[87]J. P. Castera, thesis, Orsay, 1977.
[88]G. Hepner, Appl. Opt. **14**, 1479 (1975).
[89]G. Hepner,J. P. Castera, and B. Desormiere, Physica (Utrecht) Ser. B and C **89**, 264 (1977).
[90]G. A. Smolenskiĭ, É. P. Stinser, and A. N. Ageev, Pis'ma Zh. Tekh. Fiz. **2**, 641 (1976) [Sov. Tech. Phys. Lett. **2**, 251 (1976)].
[91]É. P. Stinser, A. N. Ageev, andS. A. Mironov, *ibid.* **3**, 913 (1977) [Sov. Tech. Phys. Lett. **3**, 373 (1977)].
[92]J. Warner, Appl. Opt. **13**, 1001 (1974)
[93]J. Daval, B. Ferrand, and D. Challeton, Mater. Res. Bull. **11**, 1031 (1976).
[94]P. Anizan, G. Moisan, and M. Monerie, *ibid.*, p. 1511.
[95]S. Rashleigh, Opt. and Quantum Electron. **8**, 241 (1976).
[96]J. Warner, IEEE Trans. Microwave Theory Tech. **MTT-21**, 769 (1973).
[97]F. Auracher and H. H. Witte, Opt. Commun. **13**, 435 (1975).
[98]S. Yamamoto and t. Makimoto, J. Appl. Phys. **47**, 4056 (1976).
[99]G. A. Smolenskiĭ, S. A. Mironov, and A. N. Ageev, Pis'ma Zh. Tekh. Fiz. **3**, 284 (1977) [Sov. Tech. Phys. Lett. **3**, 114 (1977)].
[100]K. Kitayama and N. Kumagai, IEEE Trans. Microwave Theory Tech. **MTT-25**, 567 (1977).
[101]J. P. Castéra and G. Hepner, Appl. Opt. **16**, 2031 (1977); IEEE Trans. Magn. **MAG-13**, 1583 (1977).
[102]G. A. Smolenskiĭ, É. P. Stinser, and A. N. Ageev, Izv. Akad. Nauk SSSR Ser. Fiz. **43**, 287 (1979).
[103]M. Abe, M. Gomi, and S. Nomura, see Ref. 26a, p. 782; Jpn. J. Appl. Phys. **21**, 85 (1982).
[104]Y. Suematsu, Appl. Phys. Lett. **21**, 291 (1972); S. Wright, Electron. Lett. **15**, 510 (1979).
[105]G. Hepner and J. P. Castéra, Appl. Opt. **15**, 1683 (1976).
[106]G. F. Santer and M. M. Hanson, Appl. Phys. Lett. **30**, 11 (1977).
[107]P. Hlawiczka, Electron. Lett. **15**, 109 (1979).
[108]A. D. Fisher, J. N. Lee, and E. S. Gaynor, Appl. Phys. Lett. **41**, 779 (1982).
[109]R. C. Le Craw, D. L. Wood, J. F. Dillon, and J. P. Remeika, *ibid.* 7, 27 (1965); IEEE Trans. Magn. **MAG-2**, 304 (1966).
[110]A. M. Prokhorov, ed., Spravochnik po lazeram (Handbook of Lasers), Vol. 2, Sov. Radio, M., 1978.

Translated by M. V. King